

AD \_\_\_\_\_

Award Number: W81XWH-04-1-0802

TITLE: Bioenergetic Approaches and Inflammation in MPTP Toxicity

PRINCIPAL INVESTIGATOR: M. Flint Beal, M.D.

CONTRACTING ORGANIZATION: Weill Medical College of Cornell University  
New York, NY 10021

REPORT DATE: September 2005

TYPE OF REPORT: Annual

PREPARED FOR: U.S. Army Medical Research and Materiel Command  
Fort Detrick, Maryland 21702-5012

DISTRIBUTION STATEMENT: Approved for Public Release;  
Distribution Unlimited

The views, opinions and/or findings contained in this report are those of the author(s) and should not be construed as an official Department of the Army position, policy or decision unless so designated by other documentation.

20051107 291

# REPORT DOCUMENTATION PAGE

Form Approved  
OMB No. 0704-0188

Public reporting burden for this collection of information is estimated to average 1 hour per response, including the time for reviewing instructions, searching existing data sources, gathering and maintaining the data needed, and completing and reviewing this collection of information. Send comments regarding this burden estimate or any other aspect of this collection of information, including suggestions for reducing this burden to Department of Defense, Washington Headquarters Services, Directorate for Information Operations and Reports (0704-0188), 1215 Jefferson Davis Highway, Suite 1204, Arlington, VA 22202-4302. Respondents should be aware that notwithstanding any other provision of law, no person shall be subject to any penalty for failing to comply with a collection of information if it does not display a currently valid OMB control number. PLEASE DO NOT RETURN YOUR FORM TO THE ABOVE ADDRESS.

1. REPORT DATE 01-09-2005		2. REPORT TYPE Annual		3. DATES COVERED 1 Sep 2004 – 31 Aug 2005	
4. TITLE AND SUBTITLE  Bioenergetic Approaches and Inflammation in MPTP Toxicity				5a. CONTRACT NUMBER	
				5b. GRANT NUMBER W81XWH-04-1-0802	
				5c. PROGRAM ELEMENT NUMBER	
6. AUTHOR(S)  M. Flint Beal, M.D.				5d. PROJECT NUMBER	
				5e. TASK NUMBER	
				5f. WORK UNIT NUMBER	
7. PERFORMING ORGANIZATION NAME(S) AND ADDRESS(ES)  Weill Medical College of Cornell University New York, NY 10021				8. PERFORMING ORGANIZATION REPORT NUMBER	
9. SPONSORING / MONITORING AGENCY NAME(S) AND ADDRESS(ES) U.S. Army Medical Research and Materiel Command Fort Detrick, Maryland 21702-5012				10. SPONSOR/MONITOR'S ACRONYM(S)	
				11. SPONSOR/MONITOR'S REPORT NUMBER(S)	
12. DISTRIBUTION / AVAILABILITY STATEMENT Approved for Public Release; Distribution Unlimited					
13. SUPPLEMENTARY NOTES					
14. ABSTRACT  NOT PROVIDED					
15. SUBJECT TERMS NOT PROVIDED					
16. SECURITY CLASSIFICATION OF:			17. LIMITATION OF ABSTRACT	18. NUMBER OF PAGES	19a. NAME OF RESPONSIBLE PERSON
a. REPORT U	b. ABSTRACT U	c. THIS PAGE U			USAMRMC
			UU	30	19b. TELEPHONE NUMBER (include area code)

## Table of Contents

Cover.....	1
SF 298.....	2
Table of Contents.....	3
Introduction.....	4
Body.....	5
Key Research Accomplishments.....	8
Reportable Outcomes.....	9
Conclusions.....	10
References.....	11
Appendices.....	12

#### 4. INTRODUCTION

We wish to continue to examine a number of new neuroprotective agents in the MPTP model of PD, which act by inhibiting the mitochondrial permeability transition (MPT). We also wish to utilize metabolomic profiling to identify novel biomarkers for PD and to investigate whether these occur in animal models of PD. We will develop and characterize a new animal model of PD making a knockout of PINK1, which is a nuclear-encoded kinase localized to mitochondria, and which causes autosomal recessive PD. Lastly, we wish to study the effects of human dopaminergic stem cells in the 6-hydroxy-dopamine model of PD.

##### Outline of Research Goals:

Task 1: To determine the ability of pharmacologic agents to prevent MPTP neurotoxicity (months 1 – 24).

1. Examine neuroprotective effects of phosphodiesterase IV inhibitor rolipram on MPTP.
2. Examine neuroprotective effects of mitochondrial targeted antioxidants (SS02 and SS31), which inhibit the MPT.
3. Examine neuroprotective effects of celastrol and promethazine on MPTP.
4. Examine a novel form of Coenzyme Q<sub>10</sub> (CoQ<sub>10</sub>) in the MPTP model of PD.
5. Examine the role of caspase 3 activation in activation of microglia and MPTP toxicity.

Task 2: To develop a new transgenic mouse model of PD by knocking out PINK1, a protein in which mutations cause autosomal recessive PD (months 1-48).

Task 3: To utilize metabolomic profiling to develop biomarkers for PD. We will utilize metabolomic profiling to study patients with PD and animal models of PD (months 1-48).

Task 4. To determine the efficacy of human dopaminergic stem cells in the 6-hydroxydopamine (6-OHDA) model of PD (months 6 -24).

Many lines of investigation pointed to mitochondria dysfunction as an important pathogenic event in PD. In postmortem PD patients, mitochondria impairment and oxidative damage were detected (Jenner and Olanow 1998; Beal 2003). Three mitochondrial complex I inhibitors (MPTP, rotenone, and paraquat) induced parkinsonian syndrome and pathology (Dauer and Przedborski 2003).

## 5. BODY

**Task 1:** To determine the ability of pharmacologic agents to prevent MPTP neurotoxicity (months 1 – 24).

### 1. Examine neuroprotective effects of phosphodiesterase IV inhibitor rolipram on MPTP.

We completed studies with the phosphodiesterase inhibitor rolipram. We administered rolipram at either 1.2 mg/kg or 2.5 mg/kg. This was done in C57 bl/6 mice. We then evaluated its effects on protecting against dopamine depletion and the preservation of tyrosine hydroxylase positive neurons in the substantia nigra. We found that there was significant protection at both doses of rolipram. There was no effect on MPP<sup>+</sup> levels suggesting that the effects were not mediated by an alteration in processing. A dose of 5 mg/kg exerted some toxicity. These results provide further evidence that rolipram may be a useful agent for neuroprotection in Parkinson's Disease (PD).

### 2. Examine neuroprotective effects of mitochondrial targeted antioxidants (SS02 and SS31), which inhibit the MPT.

We carried out initial studies of the mitochondrial targeted antioxidants SSO2 and SS31. We have found that these agents show significant protection. These studies are still ongoing.

### 3. Examine neuroprotective effects of celastrol and promethazine on MPTP.

We completed studies of celastrol. Celastrol is an interesting compound, which was initially identified in a screen of 1000 FDA approved compounds for neuroprotective effects. Celastrol has direct effects on heat shock transcription factor 1. It is a very potent inducer of this transcription factor, which then modulates the expression of a number of chaperone genes including HSP70. Celastrol also has both anti-inflammatory and antioxidant effects. We found that celastrol attenuated dopaminergic neuron loss induced by MPTP in the substantia nigra pars compacta. Mice that received MPTP alone sustained a 50% loss of dopaminergic neurons, which was significantly diminished by treatment with celastrol. This protection was essentially complete. MPTP also induced depletion of striatal dopamine. Celastrol significantly protected against MPTP induced loss of dopamine as well as of its metabolite 3,4-dihydroxyphenylacetic acid. Celastrol was shown to induce HSP70. We showed that after administration of celastrol HSP70 immunostaining was strongly increased in the SNPC of the celastrol PBS treated mice. It was almost absent one week after completion of MPTP treatment. However, when celastrol was administered with MPTP, there was a marked increase in HSP70 immunolabelling. We used double immunofluorescence to show that there was co-localization of HSP70 with tyrosine hydroxylase. HSP70 was observable in the cytoplasm as well as in the nucleus of the dopaminergic neurons. Quantification showed that there was translocation of HSP70 into the nucleus. The nuclear translocation of

inducible HSP70 is necessary for the generation of nuclear expressed HSP70. We examined the effects of celastrol on the inflammatory cytokine TNF $\alpha$ . The number of TNF $\alpha$  immunoreactive neurons were significantly lower in the celastrol MPTP treated mice as compared to MPTP alone. TNF $\alpha$  production activates the transcription factor of NF $\kappa$ b. We found that MPTP treatment increased NF $\kappa$ b immunoreactivity in the SNPC and this was attenuated by celastrol treatment. We also found that celastrol also significantly reduced striatal lesion volumes produced by 3-nitropropionic acid (3-NP) in rats and it induced HSP70 in the striata of 3-NP rats. This was confirmed both by immunocytochemistry as well as by measurement of HSP70 levels with ELISA.

We also carried out studies of promethazine. Promethazine is a compound which was identified in the screen of 1000 FDA approved compounds. It was shown to have neuroprotective effects in a model of ischemia and reperfusion. It is a potent inhibitor of activation of the mitochondrial permeability transition (MPT). It delayed calcium induced MPT without impairing mitochondrial physiology. In brain cells *in vivo*, promethazine has been shown to accumulate into mitochondria and vesicles. We administered it at several dose levels to determine whether it could protect against MPTP induced loss of dopaminergic neurons. Promethazine treatment had no effect on MPP<sup>+</sup> concentrations on mouse striatum and it had no effect on inhibition on mitochondrial complex 1 in the striatum. It however, protected dopaminergic neurons against MPTP induced loss. In experiments with isolated brain mitochondria, promethazine impartially prevented and reversed MPP<sup>+</sup> induced depolarization of membrane potential. It inhibited the permeability transition in both brain and liver mitochondria. It, therefore, appears to be a promising potential agent for treatment of PD.

#### 4. Examine a novel form of Coenzyme Q<sub>10</sub> (CoQ<sub>10</sub>) in the MPTP model of PD.

We carried out studies using triacetyluridine as a neuroprotective agent. Triacetyluridine can improve energy metabolism in the brain. It significantly increases uridine levels. Uridine is necessary for mitochondrial function in cells, which have been depleted of mitochondrial DNA. Oral administration of triacetyluridine resulted in a significant protection against loss of tyrosine hydroxylase positive neurons in the substantia nigra produced by MPTP. It also is protective against loss of dopamine and its metabolites. We are continuing studies of a novel form of coenzyme Q<sub>10</sub> in the MPTP model of PD.

#### 5. Examine the role of caspase 3 activation in activation of microglia and MPTP toxicity.

These studies are ongoing.

**Task 2:** To develop a new transgenic mouse model of PD by knocking out PINK1, a protein in which mutations cause autosomal recessive PD (months 1-48).

With regard to task 2, we have generated PINK1 knockout mice. Correctly target ES cells were used for injection to generate the PINK1 knockout mouse founders. Founders in which the target allele transmitted to the germ line, were used to breed the homozygosity. We used a combination of PCR and sequencing to confirm the correct genetic manipulation. Primer Neo3A and 26 will amplify a 193 base per fragment only

from the targeted allele. We tested the founders in their F1 mice by PCR tail DNA with primer Neo3A and primer 26. The correct sized PCR fragments were obtained from knockout mice but not the wildtype control mice. These PCR products were sequenced to confirm the fragment is a composite of the Neo cassette in PINK1 exon 5. We, therefore, have clearly generated PINK1 deficient mice. We also used a Southern blot with the fragment of the targeting cassette has a probe. This showed only one hybridization signal of the expected size was detected.

**Task 3:** To utilize metabolomic profiling to develop biomarkers for PD. We will utilize metabolomic profiling to study patients with PD and animal models of PD (months 1-48). We are continuing to collect samples from metabolomic profiling to develop biomarkers for PD. These studies are ongoing.

**Task 4:** To determine the efficacy of human dopaminergic stem cells in the 6-hydroxydopamine (6-OHDA) model of PD (months 6 -24).

With regard to task, we are continuing our studies of the efficacy of human dopaminergic stem cells in the 6-hydroxy dopamine model of PD. These studies will take approximately 2 years to complete.

## **KEY RESEARCH ACCOMPLISHMENTS**

- a. The finding that the phosphodiesterase inhibitor rolipram exerts neuroprotective effects in the MPTP model of PD.
- b. The finding that both celastrol and promethazine exert strong neuroprotective effects in the MPTP model of PD.
- c. The finding that triacetyluridine is neuroprotective in the MPTP model of PD.
- d. The development of PINK1 knockout mice.

## **REPORTABLE OUTCOMES**

Cleren C, Calingasan NY, Chen J, Beal MF. Celastrol protects against MPTP- and 3-nitropropionic acid-induced neurotoxicity. *J Neurochem* 2005;94:995-1004

Cleren C, Starkov AA, Calingasan NY, Lorenzo BJ, Chen J, Beal MF. Promethazine protects against 1-methyl-4-phenyl-1,2,3,6-tetrahydropyridine neurotoxicity. *Neurobiol of Dis* 2005;

## **CONCLUSIONS**

We have made considerable progress in our research goals. We have demonstrated neuroprotective effects of rolipram, triacetyluridine celastrol and promethazine in the MPTP model of PD. We have developed PINK1 knockout mice. We are continuing studies of other neuroprotective agents, metabolomics and neural stem cells.

## REFERENCES

None

## APPENDICES

Cleren C, Calingasan NY, Chen J, Beal MF. Celastrol protects against MPTP- and 3-nitropropionic acid-induced neurotoxicity. *J Neurochem* 2005;94:995-1004

Cleren C, Starkov AA, Calingasan NY, Lorenzo BJ, Chen J, Beal MF. Promethazine protects against 1-methyl-4-phenyl-1,2,3,6-tetrahydropyridine neurotoxicity. *Neurobiol of Dis* 2005;

## Celastrol protects against MPTP- and 3-nitropropionic acid-induced neurotoxicity

Carine Cleren, Noel Y. Calingasan, Junya Chen and M. Flint Beal

Department of Neurology and Neuroscience, Weill Medical College of Cornell University, New York-Presbyterian Hospital, New York, New York, USA

### Abstract

Oxidative stress and inflammation are implicated in neurodegenerative diseases including Parkinson's disease (PD) and Huntington's disease (HD). Celastrol is a potent anti-inflammatory and antioxidant compound extracted from a perennial creeping plant belonging to the *Celastraceae* family. Celastrol is known to prevent the production of proinflammatory cytokines, inducible nitric oxide synthase and lipid peroxidation. Mice were treated with celastrol before and after injections of MPTP, a dopaminergic neurotoxin, which produces a model of PD. A 48% loss of dopaminergic neurons induced by MPTP in the substantia nigra pars compacta was significantly attenuated by

celastrol treatment. Moreover, celastrol treatment significantly reduced the depletion in dopamine concentration induced by MPTP. Similarly, celastrol significantly decreased the striatal lesion volume induced by 3-nitropropionic acid, a neurotoxin used to model HD in rats. Celastrol induced heat shock protein 70 within dopaminergic neurons and decreased tumor necrosis factor- $\alpha$  and nuclear factor  $\kappa$  B immunostainings as well as astrogliosis. Celastrol is therefore a promising neuroprotective agent for the treatment of PD and HD.

**Keywords:** celastrol, gliosis, heat shock protein 70, Huntington, inflammation, Parkinson.

*J. Neurochem.* (2005) **94**, 995–1004.

Parkinson's disease (PD) is a progressive neurodegenerative disorder which most commonly manifests between the fifth and seventh decade with bradykinesia, tremor and postural rigidity. At disease onset, a large proportion of dopaminergic neurons in the substantia nigra pars compacta (SNpc) have degenerated, resulting in a depletion of dopamine (DA) in the striatum (Hornykiewicz 1966). The causes of PD remain unknown but substantial evidence suggests an etiology involving both genetic and environmental factors (Greenamyre and Hastings 2004; Moore *et al.* 2004).

Huntington's disease (HD) is an inherited autosomal dominant neurodegenerative disorder which is characterized by choreiform abnormal movements, cognitive deficits and psychiatric manifestations and is associated with preferential degeneration of medium spiny GABAergic neurons located in the striatum (Harper 1991). Whereas the genetic defect responsible for HD is clearly identified as an expansion of a polyglutamine sequence within the huntingtin protein (The Huntington's Disease Collaborative Research Group 1993), many of the pathological mechanisms linking the mutant protein to the neurodegeneration remain highly speculative. The pathogenesis of PD and HD appears to involve oxidative stress, mitochondrial dysfunction, microglial activation and production of proinflammatory cytokines (Blum *et al.* 2001;

Deckel 2001; Orr *et al.* 2002; Beal 2003; Beal and Ferrante 2004).

Administration of the succinate dehydrogenase inhibitor 3-nitropropionic acid (3-NP) produces, in rodents and primates, the principal features of HD (Brouillet *et al.* 1998; Blum *et al.* 2002). There is degeneration of striatal medium-sized spiny GABAergic neurons (Beal *et al.* 1993), abnormal movements and cognitive deficits (Brouillet *et al.* 1999; El Massioui *et al.* 2001). Administration of MPTP, in primates and rodents, reproduces the characteristic degeneration of nigrostriatal dopaminergic neurons with a decrease in striatal DA (Heikkila *et al.* 1984; Ramsay and Singer

Received December 22, 2004; revised manuscript received April 5, 2005; accepted April 7, 2005.

Address correspondence and reprint requests to Dr M. Flint Beal, Department of Neurology and Neuroscience, Weill Medical College of Cornell University, 525 East 68th Street, Room F-610, New York, NY, USA. E-mail: fbeal@med.cornell.edu

**Abbreviations used:** DA, dopamine; DMSO, dimethylsulfoxide; HD, Huntington's disease; HSP, heat shock protein; I $\kappa$ B $\alpha$ , inhibitor alpha; NF $\kappa$ B, nuclear factor  $\kappa$  B; 3-NP, 3-nitropropionic acid; OSA, octane-sulfonic acid; PBS, phosphate-buffered saline; PD, Parkinson's disease; SNpc, substantia nigra pars compacta; TH, tyrosine hydroxylase; TNF- $\alpha$ , tumor necrosis factor- $\alpha$ .

1986). Both toxins lead to mitochondrial dysfunction, production of oxidative stress, release of proinflammatory cytokines and gliosis (Brouillet *et al.* 1999; Blum *et al.* 2001).

Celastrol, a triterpene, is a potent anti-inflammatory and antioxidant that is extracted from the root bark of an ivy-like vine, *Tripterygium wilfordii* Hook, which belongs to the family of *Celastraceae*. In China, this plant has a long history of use in traditional medicine for treating fever and joint pain. Studies have shown that celastrol suppresses microglial activation, pro-inflammatory cytokine production and the formation of inducible nitric oxide (Allison *et al.* 2001). Celastrol has been shown to strongly inhibit lipid peroxidation induced by ADP and  $\text{Fe}^{2+}$  (Sassa *et al.* 1990). In rat liver mitochondrial membranes, its  $\text{IC}_{50}$  was 7  $\mu\text{M}$  and it was 15 times more effective than the most commonly used antiperoxidative agent,  $\alpha$ -tocopherol (Sassa *et al.* 1990). The dienonephenol moiety of celastrol inhibits the peroxidation of outer and inner mitochondrial membranes by direct radical scavenging, while the anionic carboxyl group prevents the attack of oxygen radicals on the inner membrane by increasing its negative surface charge (Sassa *et al.* 1994). Celastrol is of great interest as it is a compound which could be easily placed into human clinical trials due to its lack of toxicity. We investigated the neuroprotective effects of celastrol in rodent models of PD and HD.

## Materials and methods

### Materials

All reagents were purchased from Sigma (St Louis, MO, USA) except celastrol which was purchased from Microsource (Gaylordsville, CT, USA) and dissolved in a mixture of dimethylsulfoxide (DMSO) and cremophore (10%/90%). Despite the fact that this mixture was always used as a solvent, we only refer to 'DMSO' in order to make the figures and text more concise. 3-NP was dissolved in distilled water and the pH was adjusted to 7.4. MPTP was dissolved in phosphate-buffered saline (PBS). 2,3,5-triphenyl tetrazolium chloride was diluted (2%) in distilled water.

### Animals and procedures

The experiments were carried out on mice and rats in accordance with the NIH Guide for the Care and Use of Laboratory Animals. All procedures were approved by the local Animal Care and Use Committee. Mice (four per cage) and rats (two per cage) were maintained in a temperature/humidity-controlled environment under a 12-h light/dark cycle with free access to food and water. Male Swiss Webster mice (8–12 mice per group, 12 weeks old) were injected with celastrol (3 mg/kg, i.p.) or 'DMSO' (10% DMSO/90% cremophore; 10 mL/kg) 12 h before and 12 h after receiving the first MPTP injection (15 mg/kg, i.p. each 2 h  $\times$  4 doses) or PBS injections (10 mL/kg). Therefore, each celastrol/MPTP-treated mouse received two celastrol injections (3 mg/kg, i.p.) 24 h apart and four MPTP injections (15 mg/kg, i.p.) 2 h apart. The last MPTP injection was performed 6 h after the first injection. Mice were

killed 7 days later by cervical dislocation. Male Lewis rats (12 weeks old) were anesthetized with isoflurane before being subcutaneously implanted with osmotic minipumps (2ML1 Alzet pump) containing 3-NP. Rats were continuously infused with 3-NP for 5 days at a daily dose of 54 mg/kg (Ouay *et al.* 2000). Beginning 24 h after the surgery, rats were injected twice a day with celastrol (3 mg/kg/dose, i.p.) until killing. Rats were killed 5 days after the surgery.

### HPLC measurement of dopamine and metabolites

For measurement of DA and its metabolites, dissected striata were immediately frozen on dry ice and stored at  $-80^{\circ}\text{C}$ . Tissues were sonicated and centrifuged in chilled 0.1 M perchloric acid (about 100  $\mu\text{L}$ /mg tissue). The supernatant fluids were taken for measurements of levels of DA and its metabolites 3,4-dihydroxyphenylacetic acid and homovanillic acid by HPLC, as modified from our previously described method (Beal *et al.* 1990). Briefly, 10  $\mu\text{L}$  supernatant fluid was isocratically eluted through an  $80 \times 4.6\text{-mm}$  C18 column (ESA, Inc., Chelmsford, MA, USA) with a mobile phase containing 75 mM of  $\text{NaH}_2\text{PO}_4$ , 1.5 mM octanesulfonic acid (OSA), 5% acetonitrile (pH 3) and detected by a two-channel Coulchem II electrochemical detector (ESA, Inc.). The flow rate was 1 mL/min. Concentrations of DA and its metabolites are expressed as nanograms per milligram of protein. The protein concentrations of tissue homogenates were measured with the protein analyse protocol (Bio-Rad Laboratories, Hercules, CA, USA) and HTS7000+ plate reader (Perkin Elmer, Norwalk, CT, USA).

### Measurement of inducible heat shock protein 70 levels by ELISA

Dissected mouse substantia nigra as well as rat striata were immediately frozen on dry ice and stored at  $-80^{\circ}\text{C}$ . The expression of heat shock protein (HSP)70 was measured using a StressXpress HSP70 ELISA kit (Stressgen Biotechnologies, Victoria, BC, Canada) according to the manufacturer's instructions with some modifications, i.e. the frozen tissue was placed in a 1-mL Dounce homogenizer with 250  $\mu\text{L}$  (substantia nigra) or 500  $\mu\text{L}$  (striata) of extraction reagent and homogenized manually with 15 strokes of the pestle. Samples were not diluted and were incubated for 3 h.

### Histological and stereological analyses

Fresh brains were fixed by immersion in 4% paraformaldehyde overnight at  $4^{\circ}\text{C}$ . Before sectioning, the tissues were placed in 30% glucose overnight at  $4^{\circ}\text{C}$  for cryoprotection. Serial coronal sections (50  $\mu\text{m}$  thick) were cut through the substantia nigra (mice) or the striatum (rats) using a cryostat. In the mice, two sets consisting of eight sections each, 100  $\mu\text{m}$  apart, were prepared. One set of sections was used for Nissl staining and the other was processed for tyrosine hydroxylase (TH) immunohistochemistry using the avidin-biotin peroxidase technique (Vectastain ABC kit; Vector Laboratories, Burlingame, CA, USA). A rabbit anti-TH affinity-purified antibody (1 : 3000; Chemicon, Temecula, CA, USA) was used. The numbers of Nissl-stained or TH-immunoreactive cells in the SNpc were counted using the optical fractionator (West *et al.* 1991). Analysis was performed using a system consisting of an Eclipse E600 microscope (Nikon, Melville, NY, USA) equipped with a computer-controlled LEP BioPoint motorized stage, DEI-750 video camera, Dimension 4300 computer (Dell, Round Rock, TX, USA).

and the Stereo Investigator (v. 4.35) software program (Microbrightfield, Burlington, VT, USA). Tissue sections were examined using a Plan Apo 100× objective lens (Nikon) with a 1.4 numerical aperture. The size of the  $x$ - $y$  sampling grid was 140  $\mu\text{m}$ . The counting frame thickness was 14  $\mu\text{m}$  and the counting frame area was 4900  $\mu\text{m}^2$ . The coefficient of error and coefficient of variation were also determined. A separate set of sections was used for immunohistochemistry using antibodies detailed in Table 1.

Double label immunofluorescence was employed to demonstrate colocalization of TH and HSP70. For the quantification in the SNpc of HSP70 immunoreactivity in nuclear and cytoplasmic compartments, three sections per mouse (100  $\mu\text{m}$  apart) were analysed ( $n = 5$  mice per group). The numbers of neurons per section with predominant staining in either the nuclei or perikarya were determined. Data are expressed as a percentage of neurons with intense nuclear staining. The numbers of tumor necrosis factor- $\alpha$  (TNF- $\alpha$ )-immunoreactive cells in the substantia nigra of mice were estimated stereologically using the optical fractionator technique as described for the TH-positive cell counts. Only intensely stained cells were counted.

For 3-NP lesion volume analysis, brains were sectioned at 2-mm intervals. Slices were immediately placed in 2% 2,3,5-triphenyl tetrazolium chloride in the dark for 30 min and then stored, protected from light, in 4% paraformaldehyde. Lesions, noted by pale staining, were evaluated on the surface of each section using a Microcomputer Image Device (Imaging Research Inc., St. Catherine, ON, Canada). Lesion volumes were calculated by multiplying the lesion area by the slice thickness. We previously showed that these measurements exhibit no significant differences from those obtained with Nissl staining (Schulz *et al.* 1995).

#### Statistical analysis

All data were computed in a database (Instat<sup>®</sup> software; GraphPad Software Inc., San Diego, CA, USA) and expressed as mean  $\pm$  SEM. Differences between groups and interaction between treatments were assessed by Student's  $t$ -test (unpaired) or by a one-way ANOVA followed, when appropriate, by a Student-Newman Keuls post-hoc test. A probability level of 5% ( $p < 0.05$ ) was considered significant.

## Results

### Celastrol attenuated dopaminergic neuron loss induced by MPTP in the substantia nigra pars compacta

Dimethylsulfoxide-treated mice that received MPTP (15 mg/kg, i.p. q 2 h  $\times$  4 doses) sustained a 48% ( $p < 0.001$ ) loss of

Nissl-immunopositive neurons and a 48% ( $p < 0.01$ ) loss of TH-immunopositive dopaminergic neurons within the SNpc compared with DMSO/PBS-treated mice (Fig. 1 and Table 2). Celastrol alone (3 mg/kg, i.p. q 12 h  $\times$  2 doses) did not have any effect on the number of Nissl-immunopositive neurons or on the number of TH-immunopositive neurons. However, celastrol treatment significantly diminished the MPTP-induced loss of SNpc neurons. Indeed, celastrol protected against the loss of Nissl- ( $p < 0.001$ ) and TH- ( $p < 0.01$ ) immunopositive neurons. This protection was strong as the number of Nissl- and TH-immunopositive neurons was not significantly different between the DMSO/PBS and celastrol/MPTP groups.

### Celastrol reduced MPTP-induced depletion of striatal dopamine levels

Celastrol alone had no effect on striatal DA levels (Fig. 2). MPTP administration induced a 37% depletion of striatal DA level compared with DMSO/PBS-treated mice ( $p < 0.001$ ). Celastrol significantly protected against the MPTP-induced depletion of striatal DA ( $p < 0.05$ ). The striatal DA levels of celastrol/MPTP-treated mice were not significantly different from those of celastrol/PBS-treated mice. MPTP treatment also induced a significant decrease in striatal 3,4-dihydroxyphenylacetic acid (–34%,  $p < 0.001$ ) and homovanillic acid (–29%,  $p < 0.001$ ). Celastrol treatment prevented the MPTP-induced 3,4-dihydroxyphenylacetic acid depletion ( $p < 0.05$ ).

### Celastrol reduction of MPTP neurotoxicity is accompanied by increased heat shock protein 70 expression in the substantia nigra pars compacta

Heat-shock chaperones such as HSP70 have been shown to confer protection in a *Drosophila* model of PD (Auluck *et al.* 2002). We therefore examined whether the protection observed could result, at least in part, from an increase in the inducible form of HSP70 by celastrol. At 1 week after two injections of celastrol (3 mg/kg, q 24 h  $\times$  2 doses), HSP70 immunostaining was strongly increased in the SNpc of celastrol/PBS-treated mice. As revealed by immunocytochemistry, the solvent 'DMSO' (10%/90%) used to dissolve celastrol also enhanced HSP70 immunostaining in the SNpc. However, the inducible form of HSP70 was almost totally

**Table 1** List of antibodies used

	Antibody	Company	Dilution
HSP70	Rabbit anti-HSP70 (HSP72) polyclonal	Stressgen Biotechnologies, Victoria, BC, Canada	1 : 2000
TNF- $\alpha$	Rabbit anti-TNF- $\alpha$ polyclonal	Calbiochem-Novabiochem Corporation, San Diego, CA, USA	1 : 100
NF $\kappa$ B	Affinity-purified rabbit anti-NF $\kappa$ B p65 polyclonal	Santa Cruz Biotechnology, Inc., Santa Cruz, CA, USA	1 : 500
CD40L	Goat anti-CD40L rabbit polyclonal	Santa Cruz Biotechnology, Inc.	1 : 1000
TH	Anti-TH	Chemicon, Temecula, CA, USA	1 : 4000

HSP, heat shock protein; NF $\kappa$ B, nuclear factor  $\kappa$  B; TH, tyrosine hydroxylase; TNF- $\alpha$ , tumor necrosis factor- $\alpha$ .

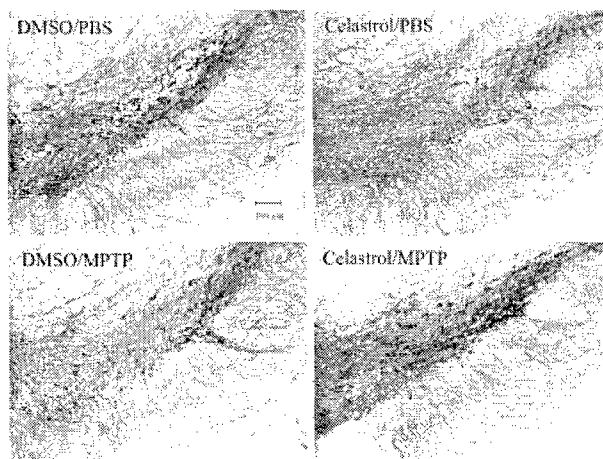


**Fig. 1** Effect of celastrol treatment on MPTP-induced loss of dopamine neurons in mice. Photomicrographs of tyrosine hydroxylase-immunostained sections through the substantia nigra pars compacta showing MPTP-induced loss of dopaminergic neurons and the neuroprotective effect afforded by celastrol. DMSO, dimethylsulfoxide; PBS, phosphate-buffered saline.

absent in DMSO/MPTP-treated mice 1 week after the treatment. In contrast to DMSO/MPTP-treated mice that only weakly express HSP70 at 1 week, celastrol/MPTP-treated mice showed increased HSP70 immunolabeling (Fig. 3a).

The observation that celastrol induced an increase in HSP70, obtained by immunohistochemistry, was confirmed by biochemistry. Measurement of inducible HSP70 by ELISA showed that 7 days after only two celastrol injections (3 mg/kg, q 24 h), the level of the inducible form of HSP70 was significantly increased in the substantia nigra ( $p < 0.05$ ). The two injections of DMSO did not significantly increase HSP70 compared with control (Fig. 3b).

**Table 2** Stereological counts of tyrosine hydroxylase- (TH) and Nissl-positive neurons (optical fractionator) in the substantia nigra pars compacta for each group

	Nissl (mean $\pm$ SEM)	TH (mean $\pm$ SEM)
DMSO/PBS	11 188 $\pm$ 408	9604 $\pm$ 419
Celastrol/PBS	11 071 $\pm$ 596	9483 $\pm$ 683
DMSO/MPTP	5760 $\pm$ 697	4975 $\pm$ 1119
compared with DMSO/PBS	$p < 0.001$	$p < 0.01$
Celastrol/MPTP	9658 $\pm$ 609	8575 $\pm$ 331
compared with DMSO/PBS	$p < 0.001$	$p < 0.001$

Celastrol prevented the loss of Nissl- ( $p < 0.001$ ) and TH- ( $p < 0.01$ ) positive neurons induced by MPTP. DMSO, dimethylsulfoxide; PBS, phosphate-buffered saline.

### Celastrol induced nuclear translocation of cytoplasmic heat shock protein 70

Double label immunofluorescence showed colocalization of HSP70 with TH, indicating that increased nigral HSP70 expression occurred within dopaminergic neurons. HSP70 was observable in the cytoplasm as well as in the nucleus of dopaminergic neurons (Fig. 3c). Quantification of HSP70 in both compartments showed that, in the SNpc of DMSO/MPTP-treated mice, 27% of HSP70 was in the nucleus while 73% remained in the cytoplasm. However, in celastrol/MPTP-treated mice, 47% of HSP70 was in the nucleus, indicating that celastrol induced a translocation of inducible HSP70 from the cytoplasm to the nucleus ( $p < 0.001$  compared with DMSO/PBS-treated mice) (Fig. 3d). The nuclear translocation of inducible HSP70 is necessary for the generation of newly expressed HSP70 (Barrett *et al.* 2004).

### Celastrol attenuated MPTP neurotoxicity by attenuating inflammation

In view of the known potent anti-inflammatory activity of celastrol, its effects on the production of TNF- $\alpha$  and nuclear factor  $\kappa$  B (NF $\kappa$ B) were investigated. Treatment with DMSO plus MPTP induced increased immunostaining for the inflammatory cytokine TNF- $\alpha$  in the SNpc (Fig. 4a). Intensely stained cells for TNF- $\alpha$  were counted stereologically in the substantia nigra (Fig. 4b). There were no intensely stained cells in control groups. The number of TNF- $\alpha$ -immunoreactive cells was significantly lower ( $p < 0.05$ ) in the celastrol/MPTP- than in the DMSO/MPTP-treated mice. During the inflammatory process, TNF- $\alpha$  production activates the transcription factor NF $\kappa$ B, inducing release of inflammatory cytokines (Ghosh and Karin 2002). In our experiment, DMSO/MPTP treatment increased NF $\kappa$ B immunoreactivity in the SNpc (Fig. 4a). Celastrol treatment reduced MPTP-induced immunoreactivity of NF $\kappa$ B, confirming that celastrol both directly and indirectly inhibits activation of different mediators of the inflammatory pathway.

### Celastrol reduced striatal lesion volumes induced by 3-nitropropionic acid in rats

Chronic delivery of 3-NP in rats via osmotic minipumps (54 mg/kg/day, s.c.) induced striatal lesions with a volume of approximately 12 mm<sup>3</sup> (Fig. 5). Celastrol treatment (3 mg/kg, i.p. q 12 h  $\times$  8 doses) significantly reduced 3-NP-induced neurodegeneration. Indeed, in celastrol/3-NP-treated rats, the lesion volume was nearly absent (0.17 mm<sup>3</sup>) and reduced by 98% ( $p < 0.05$ ) compared with DMSO/3-NP-treated rats.

### Celastrol induced heat shock protein 70 in the striata of 3-nitropropionic acid-treated rats

Heat-shock chaperones such as HSP70 have been shown to confer protection in models of HD (Dedeoglu *et al.* 2002) and polyglutamine-mediated neurodegeneration (Warrick *et al.* 1999). Therefore, we checked whether the strong

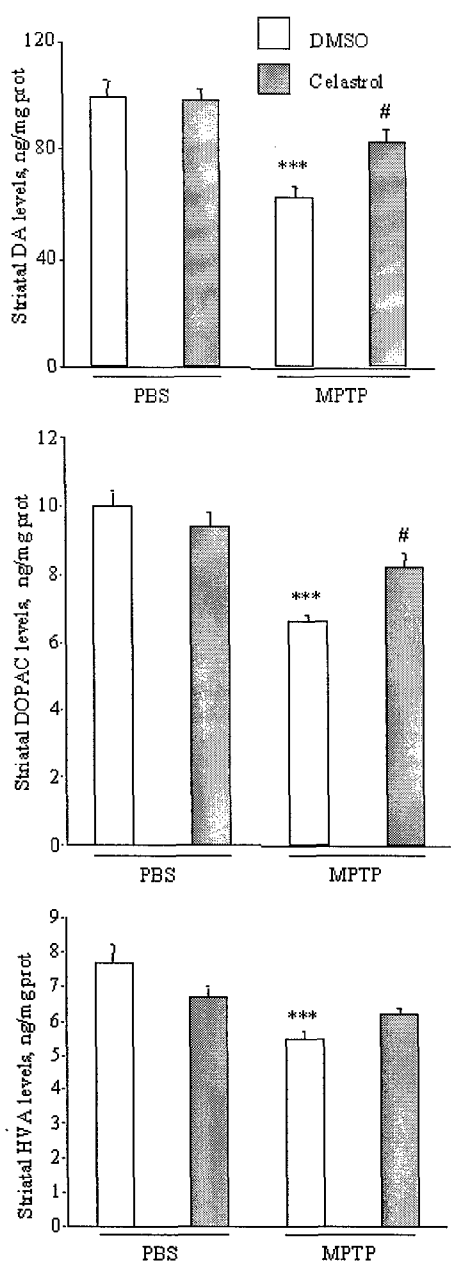


**Fig. 2** Effects of celastrol and MPTP treatments on striatal levels of dopamine (DA), 3,4-dihydroxyphenylacetic acid (DOPAC) and homovanillic acid (HVA). Celastrol treatment significantly attenuated the DA and DOPAC depletions induced by MPTP. \*\*\* $p < 0.001$  compared with dimethylsulfoxide (DMSO)/phosphate-buffered saline (PBS)-treated mice; # $p < 0.05$  compared with DMSO/MPTP-treated mice.

protection afforded by celastrol treatment resulted from HSP70 induction. The inducible form of HSP70 was weakly present in DMSO/3-NP-treated rats as assessed by immunohistochemistry (Fig. 6a). The localization of HSP70 expression in the striata of celastrol/3-NP-treated rats was similar to that observed at the site of neurodegeneration in 3-NP-treated rats. Celastrol treatment in 3-NP-

treated rats enhanced HSP70 expression by 19% ( $p < 0.05$ ) as assessed by ELISA (Fig. 6b).

### Celastrol reduces 3-nitropropionic acid-induced astrogliosis in rats

Celastrol strongly reduced 3-NP-induced neurotoxicity, probably by inducing HSP70. The results obtained with the 3-NP model are in accordance with those obtained in the MPTP model. As 3-NP is known to induce astrogliosis (Beal *et al.* 1993), we decided to examine the effects of celastrol on astrogliosis. CD40L, an inflammatory factor characteristic of astroglial cells, showed a marked staining of astrocytes in the striata of DMSO/3-NP-treated rats (Fig. 7). Celastrol treatment strongly reduced 3-NP-induced astrogliosis.

### Discussion

Celastrol protected dopaminergic neurons against the neurotoxic effects of MPTP. It prevented both the degeneration of nigrostriatal dopaminergic neurons and the loss of striatal DA induced by MPTP. Celastrol also strongly reduced the volume of striatal lesions induced by a chronic 3-NP treatment.

Heat shock protein 70, the major inducible heat shock chaperone, is induced in response to oxidative stress and neuronal injury. HSP70 plays a protective role by preventing protein misfolding and aggregation as well as oxidative injury and apoptosis (Yenari 2002). In *Drosophila* models, HSP70 has been shown to confer protection against alpha-synuclein toxicity Auluck *et al.* 2002) and polyglutamine-mediated neurodegeneration (Warrick *et al.* 1999; Bonini 2002). We found that mice overexpressing HSP70 were less sensitive to 3-NP toxicity (Dedeoglu *et al.* 2002). Moreover, a recently published study reported that HSP70 gene transfer to DA neurons, by injection of a recombinant adeno-associated virus in mice, protects against MPTP-induced neurotoxicity (Dong *et al.* 2005).

Celastrol activates heat shock transcription factor 1. It shares kinetic features with heat shock, including rapid induction within minutes and a similar magnitude of induction (Westerheide *et al.* 2004). The  $EC_{50}$  value was 3  $\mu$ M. Celastrol induced heat shock transcription factor 1 DNA binding, hyperphosphorylation of heat shock transcription factor 1 and expression of chaperone genes. The HSP70 protein and mRNA levels were similar to those which occurred with 42°C heat shock in both HeLa and neuroblastoma cells. Celastrol protected cells from subsequent lethal heat stress and decreased apoptotic cell death. Induction of HSPs is known to intervene at multiple points in the apoptotic pathway, including inhibition of c-Jun N-terminal kinase activation and prevention of cytochrome *c* release and caspase activation (Green and Kroemer 2004).

Celastrol therefore has a number of mechanisms by which it may exert neuroprotective effects, including anti-inflamma-

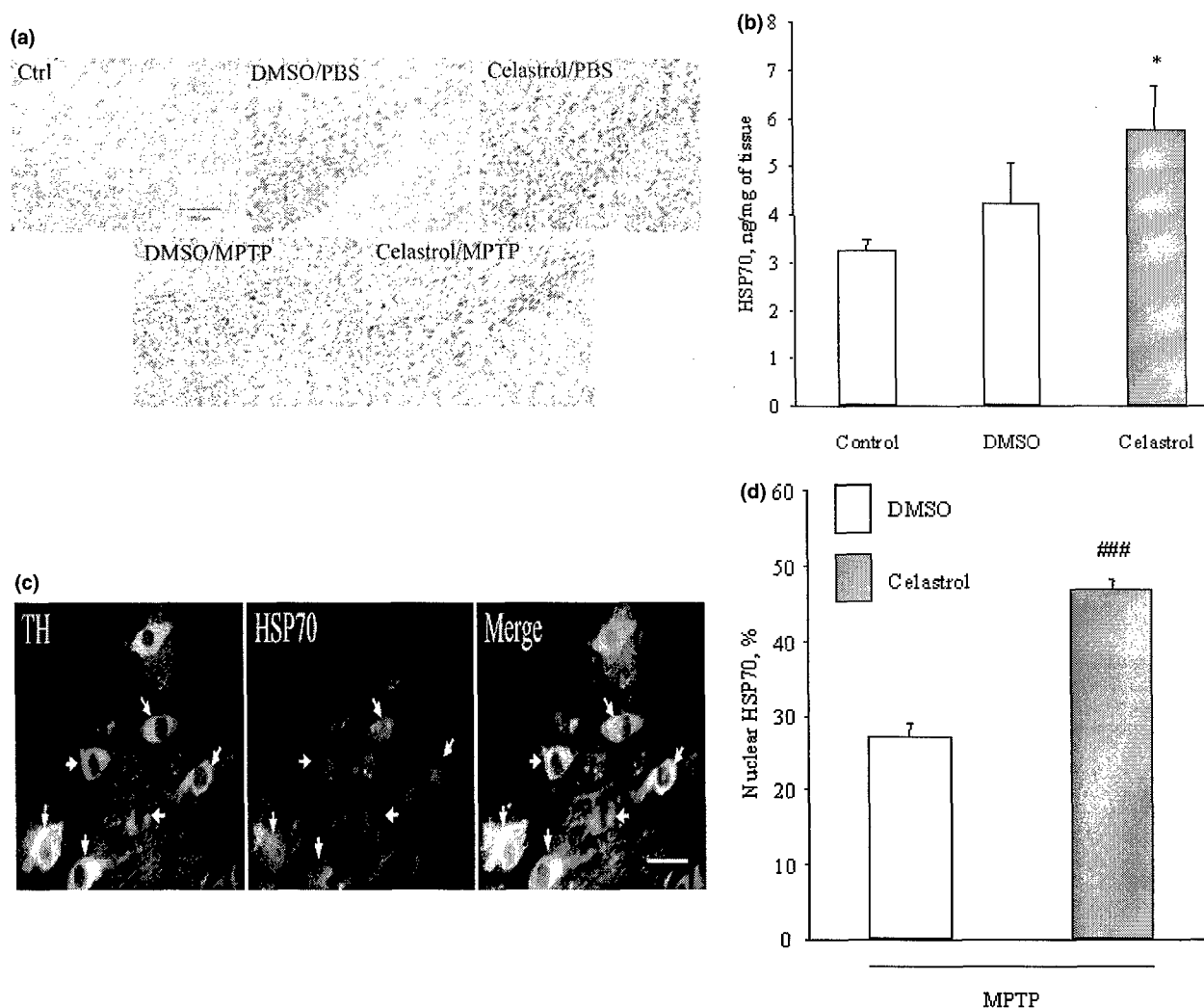


**Fig. 3** Celastrol induced an increase of heat shock protein (HSP)70 immunoreactivity and protein level in the substantia nigra as well as HSP70 nuclear translocation. (a) Inducible HSP70 immunoreactivity in the substantia nigra pars compacta (SNpc) of control (Ctrl) or MPTP-lesioned mice treated with dimethylsulfoxide (DMSO) or celastrol. Upper panel, DMSO or celastrol-induced enhancement of HSP70 immunoreactivity in phosphate-buffered saline (PBS)-treated mice. Lower panel, celastrol-induced enhancement of HSP70 immunoreactivity in MPTP-treated mice. (b) Effect of celastrol treatment on HSP70 levels in the substantia nigra. Two injections of celastrol increased HSP70 levels at 7 days. \* $p < 0.05$  compared with control mice. (c)

Colocalization of tyrosine hydroxylase (TH) (left panel) and HSP70 (middle panel) in the cytoplasm of dopaminergic neurons (arrows). The merge shows the presence of HSP70 immunoreactivity in the nucleus of TH-positive neurons. Scale bar for the right panel, 25  $\mu$ m. (d) Quantification of HSP70 immunoreactivity in the SNpc of MPTP-treated mice. The numbers of neurons with predominant staining in either the nuclei or perikarya per section were determined. Data are expressed as a percentage of neurons with intense nuclear staining. Celastrol treatment induced the nuclear translocation of HSP70 in MPTP-treated mice. ### $p < 0.001$  compared with DMSO/MPTP-treated mice.

tory and antioxidative effects and its ability to up-regulate HSPs. Indeed, some anti-inflammatory compounds are able to activate the DNA-binding activity of the heat shock transcription factor 1 and, in consequence, HSP70 expression (Morimoto and Santoro 1998). Therefore, we examined the effect of celastrol on HSP70 expression 1 week after only two injections of celastrol in mice. We observed an increase of HSP70 levels, measured by both ELISA and HSP70 immunostaining,

in the SNpc. We also observed an enhancement of HSP70 immunoreactivity 1 day after MPTP treatment (result not shown) which was reduced after 1 week. MPTP treatment (20 mg/kg, q 12 h  $\times$  4 doses) in mice was reported to result in a transient up-regulation of HSP70 expression in the substantia nigra from 4 h to 2 days after the first MPTP injection, which was no longer observable at 4 days after the treatment (Kuhn *et al.* 2003). Our results are consistent with a

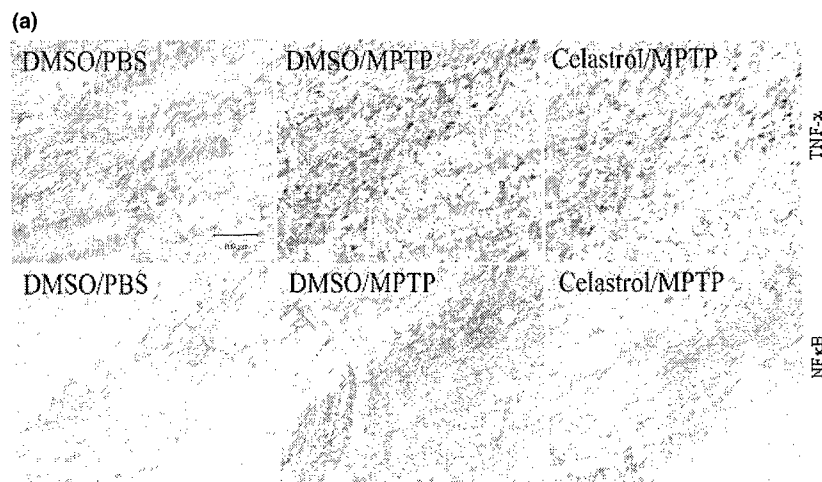


**Fig. 4** Tumor necrosis factor- $\alpha$  (TNF- $\alpha$ ) and nuclear factor  $\kappa$  B (NF $\kappa$ B) immunoreactivity in the substantia nigra pars compacta of control or MPTP-lesioned mice treated with dimethylsulfoxide (DMSO) or celastrol. (a) Celastrol attenuated the MPTP-induced increases in TNF- $\alpha$  and NF $\kappa$ B immunoreactivity in dopaminergic neurons. (b) Number of TNF- $\alpha$ -immunoreactive cells in the substantia nigra. The number of TNF- $\alpha$ -immunoreactive cells was significantly lower in the celastrol/MPTP-treated mice than in the DMSO/MPTP-treated mice. # $p < 0.05$  compared with DMSO/MPTP-treated mice. PBS, phosphate-buffered saline.

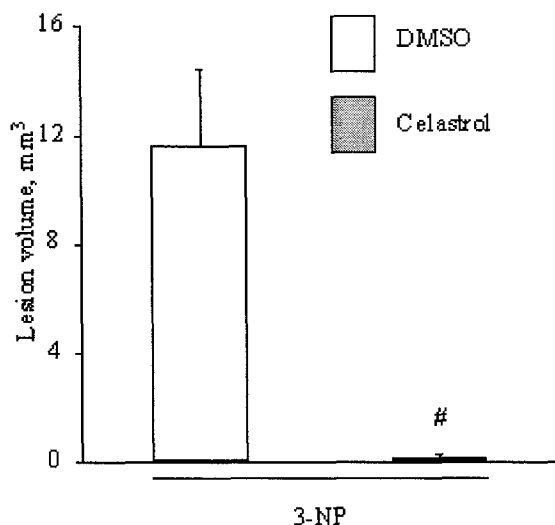
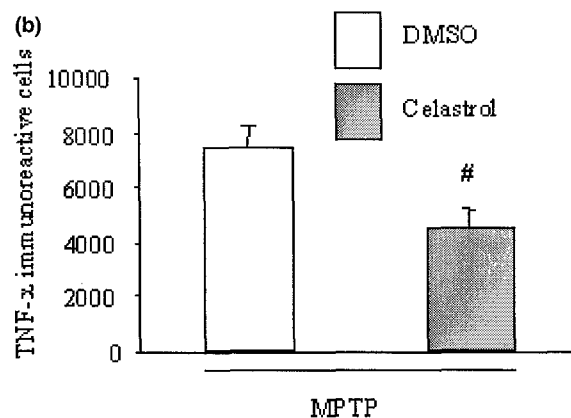


**Fig. 5** Effect of celastrol treatment on 3-nitropropionic acid (3-NP)-induced striatal lesions in rats. Celastrol strongly reduced the lesion resulting from the 3-NP treatment. # $p < 0.05$  compared with dimethylsulfoxide (DMSO)/3-NP-treated rats.

recent study showing that celastrol (3  $\mu$ M) induces HSP70 protein and mRNA levels in HeLa and neuroblastoma cells (Westerheide *et al.* 2004).

In our study, celastrol enhanced HSP70 expression in MPTP-treated mice. HSP70 may protect by regulating matrix metalloproteinases (Lee *et al.* 2004). In the brain, HSP70, by an as yet unknown mechanism, can increase Bcl-2 expression which, in turn, blocks cytochrome *c* release and subsequent effector caspase activation (Creagh *et al.* 2000; Gabai *et al.* 2002; Yenari 2002). We observed more nuclear HSP70 in celastrol/MPTP- than in DMSO/MPTP-treated mice. This difference presumably resulted from the known cytoplasm to nucleus translocation of inducible HSP70, necessary for the generation of newly expressed HSP70 (Barrett *et al.* 2004).

In their review, Malhotra and Wong (2002) reported that HSP70 prevents the activation of NF $\kappa$ B by stabilizing the Nuclear factor Kappa B inhibitor- $\alpha$  (NF $\kappa$ B-I $\kappa$ B $\alpha$ ) complex. The induction of the heat shock response before a proinflammatory signal inhibits NF $\kappa$ B activation and NF $\kappa$ B-dependent proinflammatory gene expression. Schmidt and

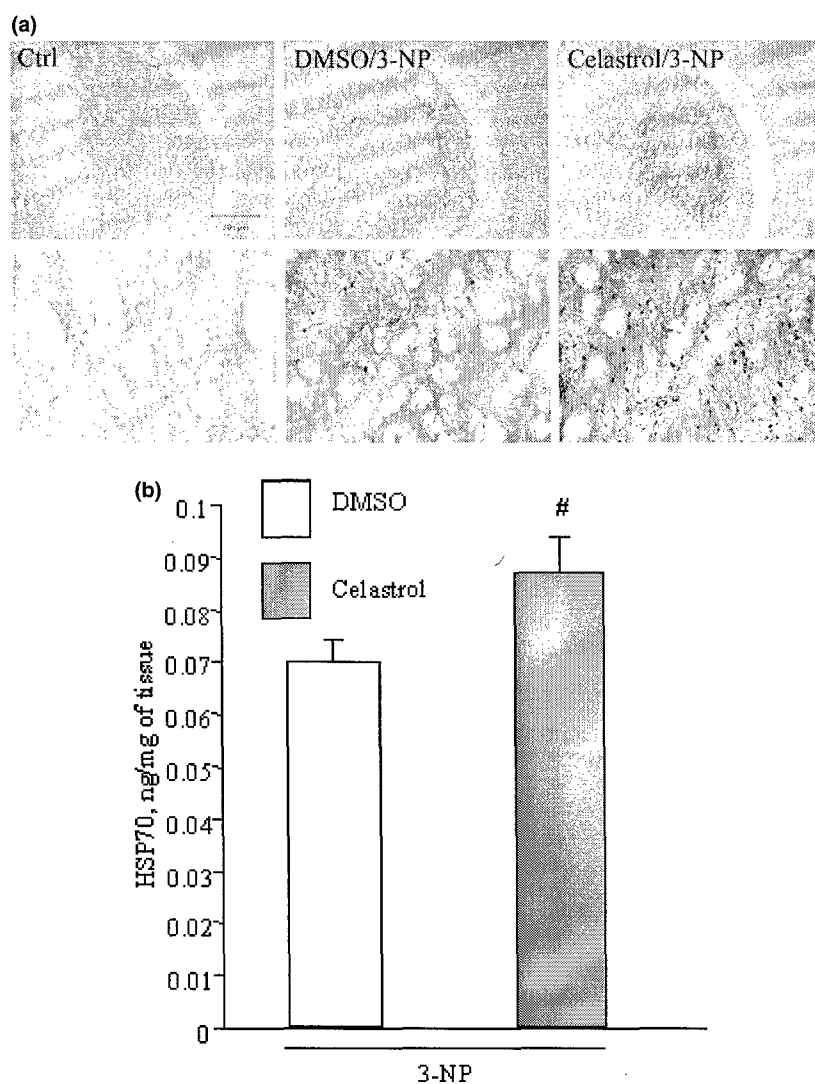


**Fig. 6** Celastrol induces heat shock protein (HSP)70 in the striatum of 3-nitropropionic acid (3-NP)-lesioned rat. (a) Upper panel, HSP70 staining was absent in control (Ctrl), moderate in the striatum of dimethylsulfoxide (DMSO)/3-NP-treated mice and most intense in celastrol/3-NP-treated mice. HSP70 labeling occurred in neurons and neuropil within the focal region vulnerable to 3-NP neurotoxicity. Lower panel, higher magnification (4 $\times$ ). (b) Celastrol treatment increased HSP70 expression in the striata of 3-NP-treated rats.  $\#p < 0.05$  compared with DMSO/3-NP-treated rats.

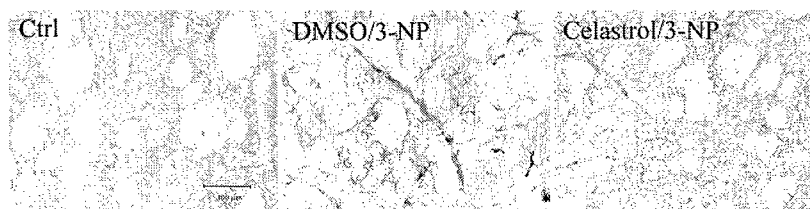


**Fig. 7** CD40L immunoreactivity in the striatum of 3-nitropropionic acid (3-NP)-lesioned rat. CD40L-immunoreactive astrocytes proliferate in dimethylsulfoxide (DMSO)/3-NP-treated rat and are attenuated by celastrol treatment. Ctrl, control.

Abdulla (1988) reported that there is a correlation between the extent of interleukin-1 $\beta$  reduction and the level of HSP induction by chemical inducers in THP-1 cells. Therefore, we investigated the effects of celastrol on inflammation. MPTP treatment induces a peak of inflammation at 7 days after its injection (Ciesielska *et al.* 2003). TNF- $\alpha$  is produced primarily by macrophages and plays a major role in the pathogenesis of inflammation. In our study, MPTP induced a marked increase in TNF- $\alpha$  immunostaining in the SNpc

7 days after MPTP administration. Celastrol treatment of MPTP-injected mice significantly reduced the MPTP-induced increase of TNF- $\alpha$ . Binding of TNF- $\alpha$  to its membrane receptor TNF-R1 activates multiple downstream signaling events including activation of caspases and NF $\kappa$ B-mediated transcription. One consequence is an up-regulation of the transcription factor NF $\kappa$ B (Ghosh and Karin 2002). To investigate whether celastrol modified TNF- $\alpha$  activity, we stained the SNpc for NF $\kappa$ B. At 7 days after the treatment,

MPTP induced an increase in NF $\kappa$ B immunoreactivity. Celastrol reduced the increase in NF $\kappa$ B staining in MPTP-treated mice. The dopaminergic neuroprotection observed in celastrol/MPTP-treated mice may therefore result, in part, from the HSP70-induced anti-inflammatory properties of celastrol, which induces a down-regulation of the transcription factor NF $\kappa$ B. This may prevent NF $\kappa$ B-induced release of cytokines, including interleukin-1 and -6.

In our experiments we observed that celastrol exerted a strong neuroprotective effect in another model of neurodegeneration. Celastrol almost completely prevented 3-NP-induced striatal lesions. As observed in the MPTP model, it is probable that celastrol protected against 3-NP toxicity by inducing HSP70. Indeed, HSP70 was induced by celastrol treatment within the upper lateral region of the striatum which is more vulnerable to 3-NP neurotoxicity. The 3-NP model has features in common with the MPTP model, such as inflammation and astrogliosis (Brouillet *et al.* 1999). TNF- $\alpha$  released from macrophages binds to astrocytes, activating them and leading to astrogliosis (Ridet *et al.* 1997). Many functions have been attributed to astroglia, including ion homeostasis, uptake of neurotransmitters and contribution to the immune system (Takuma *et al.* 2004). Astroglia also play a role in the preservation of the host tissue integrity after injury (Dervan *et al.* 2003). We examined the effects of celastrol on 3-NP-induced astrogliosis. As expected, the striata of rats treated with 3-NP showed numerous reactive astrocytes. Celastrol treatment strongly reduced 3-NP-induced astrogliosis in rats.

### Conclusions

Celastrol treatment in MPTP-treated mice was sufficient to attenuate the loss of DA and dopaminergic neurons. Celastrol also strongly reduced 3-NP-induced striatal lesions. The neuroprotective effect of celastrol may be multifactorial. Celastrol treatment induced an increase of inducible HSP70 in the substantia nigra of MPTP-treated mice, 7 days after injections, and in the striata of 3-NP-treated rats. Celastrol treatment also resulted in a strong nuclear translocation of HSP70 necessary for the generation of newly expressed HSP70. Induced HSP70 may prevent TNF- $\alpha$  and NF $\kappa$ B activation, inhibiting the release of proinflammatory cytokines and astrogliosis. We observed that celastrol treatment reduced induced inflammation and astrogliosis. HSP70 may also reduce apoptosis. Our results suggest that celastrol could play a therapeutic role in preventing and/or delaying the onset and progression of PD and HD.

### Acknowledgements

The work was supported by grants from National Institute of Neurological Disorders and Stroke, the Department of Defense, Michael J. Fox Foundation and Parkinson's Disease Foundation.

### References

- Allison A. C., Cacabelos R., Lombardi V. R., Alvarez X. A. and Vigo C. (2001) Celastrol, a potent antioxidant and anti-inflammatory drug, as a possible treatment for Alzheimer's disease. *Prog. Neuropsychopharmacol. Biol. Psychiat.* **25**, 1341–1357.
- Auluck P. K., Chan H. Y., Trojanowski J. Q., Lee V. M. and Bonini N. M. (2002) Chaperone suppression of alpha-synuclein toxicity in a Drosophila model for Parkinson's disease. *Science* **295**, 865–868.
- Barrett M. J., Alones V., Wang K. X., Phan L. and Swerdlow R. H. (2004) Mitochondria-derived oxidative stress induces a heat shock protein response. *J. Neurosci. Res.* **78**, 420–429.
- Beal M. F. (2003) Mitochondria, oxidative damage, and inflammation in Parkinson's disease. *Ann. NY Acad. Sci.* **991**, 120–131.
- Beal M. F. and Ferrante R. J. (2004) Experimental therapeutics in transgenic mouse models of Huntington's disease. *Nat. Rev. Neurosci.* **5**, 373–384.
- Beal M. F., Kowall N. W., Swartz K. J. and Ferrante R. J. (1990) Homocysteic acid lesions in rat striatum spare somatostatin-neuropeptide Y (NADPH-diaphorase) neurons. *Neurosci. Lett.* **108**, 36–42.
- Beal M. F., Brouillet E., Jenkins B. G., Ferrante R. J., Kowall N. W., Miller J. M., Storey E., Srivastava R., Rosen B. R. and Hyman B. T. (1993) Neurochemical and histologic characterization of striatal excitotoxic lesions produced by the mitochondrial toxin 3-nitropropionic acid. *J. Neurosci.* **13**, 4181–4192.
- Blum D., Torch S., Lambeng N., Nissou M., Benabid A. L., Sadoul R. and Verna J. M. (2001) Molecular pathways involved in the neurotoxicity of 6-OHDA, dopamine and MPTP: contribution to the apoptotic theory in Parkinson's disease. *Prog. Neurobiol.* **65**, 135–172.
- Blum D., Galas M. C., Gall D., Cuvelier L. and Schiffmann S. N. (2002) Striatal and cortical neurochemical changes induced by chronic metabolic compromise in the 3-nitropropionic model of Huntington's disease. *Neurobiol. Dis.* **10**, 410–426.
- Bonini N. M. (2002) Chaperoning brain degeneration. *Proc. Natl Acad. Sci. USA* **99**, S16 407–S16 411.
- Brouillet E., Guyot M. C., Mittoux V., Altaïrac S., Conde F., Palfi S. and Hantraye P. (1998) Partial inhibition of brain succinate dehydrogenase by 3-nitropropionic acid is sufficient to initiate striatal degeneration in rat. *J. Neurochem.* **70**, 794–805.
- Brouillet E., Conde F., Beal M. F. and Hantraye P. (1999) Replicating Huntington's disease phenotype in experimental animals. *Prog. Neurobiol.* **59**, 427–468.
- Ciesielska A., Joniec I., Przybylowski A., Gromadzka G., Kurkowska-Jastrzebska I., Czlonkowska A. and Czlonkowski A. (2003) Dynamics of expression of the mRNA for cytokines and inducible nitric synthase in a murine model of the Parkinson's disease. *Acta Neurobiol. Exp.* **63**, 117–126.
- Creagh E. M., Carmody R. J. and Cotter T. G. (2000) Heat shock protein 70 inhibits caspase-dependent and -independent apoptosis in Jurkat T cells. *Exp. Cell Res.* **257**, 58–66.
- Deckel A. W. (2001) Nitric oxide and nitric oxide synthase in Huntington's disease. *J. Neurosci. Res.* **64**, 99–107.
- Dedeoglu A., Ferrante R. J., Andreassen O. A., Dillmann W. H. and Beal M. F. (2002) Mice overexpressing 70-kDa heat shock protein show increased resistance to malonate and 3-nitropropionic acid. *Exp. Neurol.* **176**, 262–265.
- Dervan A. G., Totterdell S., Lau Y. S. and Meredith G. E. (2003) Altered striatal neuronal morphology is associated with astrogliosis in a chronic mouse model of Parkinson's disease. *Ann. NY Acad. Sci.* **991**, 291–294.
- Dong Z., Wolfer D. P., Lipp H. P. and Bueler H. (2005) Hsp70 gene transfer by adeno-associated virus inhibits MPTP-induced nigro-

- striatal degeneration in the mouse model of Parkinson disease. *Mol. Ther.* **11**, 80–88.
- El Massioui N., Ouay S., Cheruel F., Hantraye P. and Brouillet E. (2001) Perseverative behavior underlying attentional set-shifting deficits in rats chronically treated with the neurotoxin 3-nitropropionic acid. *Exp. Neurol.* **172**, 172–181.
- Gabai V. L., Mabuchi K., Mosser D. D. and Sherman M. Y. (2002) Hsp72 and stress kinase c-jun N-terminal kinase regulate the bid-dependent pathway in tumor necrosis factor-induced apoptosis. *Mol. Cell Biol.* **22**, 3415–3424.
- Ghosh S. and Karin M. (2002) Missing pieces in the NF-kappaB puzzle. *Cell* **109**, S81–S96.
- Green D. R. and Kroemer G. (2004) The pathophysiology of mitochondrial cell death. *Science* **305**, 626–629.
- Greenamyre J. T. and Hastings T. G. (2004) Biomedicine. Parkinson's — divergent causes, convergent mechanisms. *Science* **304**, 1120–1122.
- Harper P. S. (ed.) (1991) *Huntington's Disease*. Saunders, London.
- Heikkila R. E., Cabbat F. S., Manzino L. and Duvoisin R. C. (1984) Effects of 1-methyl-4-phenyl-1,2,5,6-tetrahydropyridine on neostriatal dopamine in mice. *Neuropharmacology* **23**, 711–713.
- Hornykiewicz O. (1966) Dopamine (3-hydroxytyramine) and brain function. *Pharmacol. Rev.* **18**, 925–964.
- Kuhn K., Wellen J., Link N., Maskri L., Lubbert H. and Stichel C. C. (2003) The mouse MPTP model: gene expression changes in dopaminergic neurons. *Eur. J. Neurosci.* **17**, 1–12.
- Lee J. E., Kim Y. J., Kim J. Y., Lee W. T., Yenari M. A. and Giffard R. G. (2004) The 70 kDa heat shock protein suppresses matrix metalloproteinases in astrocytes. *Neuroreport* **15**, 499–502.
- Malhotra V. and Wong H. R. (2002) Interactions between the heat shock response and the nuclear factor-kappaB signaling pathway. *Crit. Care Med.* **30**, S89–S95.
- Moore D. J., West A. B., Dawson V. L. and Dawson T. M. (2004) Molecular pathophysiology of Parkinson's disease. *Annu. Rev. Neurosci.* (Epub ahead of print).
- Morimoto R. I. and Santoro M. G. (1998) Stress-inducible responses and heat shock proteins: new pharmacologic targets for cytoprotection. *Nat. Biotechnol.* **16**, 833–838.
- Orr C. F., Rowe D. B. and Halliday G. M. (2002) An inflammatory review of Parkinson's disease. *Prog. Neurobiol.* **68**, 325–340.
- Ouay S., Bizat N., Altairac S., Menetrat H., Mittoux V., Conde F., Hantraye P. and Brouillet E. (2000) Major strain differences in response to chronic systemic administration of the mitochondrial toxin 3-nitropropionic acid in rats: implications for neuroprotection studies. *Neuroscience* **97**, 521–530.
- Ramsay R. R. and Singer T. P. (1986) Energy-dependent uptake of N-methyl-4-phenylpyridinium, the neurotoxic metabolite of 1-methyl-4-phenyl-1,2,3,6-tetrahydropyridine, by mitochondria. *J. Biol. Chem.* **261**, 7585–7587.
- Ridet J. L., Malhotra S. K., Privat A. and Gage F. H. (1997) Reactive astrocytes: cellular and molecular cues to biological function. *Trends Neurosci.* **20**, 570–577.
- Sassa H., Takaishi Y. and Terada H. (1990) The triterpene celastrol as a very potent inhibitor of lipid peroxidation in mitochondria. *Biochem. Biophys. Res. Commun.* **172**, 890–897.
- Sassa H., Kogure K., Takaishi Y. and Terada H. (1994) Structural basis of potent antiperoxidation activity of the triterpene celastrol in mitochondria: effect of negative membrane surface charge on lipid peroxidation. *Free Radic. Biol. Med.* **17**, 201–207.
- Schmidt J. A. and Abdulla E. (1988) Down-regulation of IL-1 beta biosynthesis by inducers of the heat-shock response. *J. Immunol.* **14**, 2027–2034.
- Schulz J. B., Henshaw D. R., Matthews R. T. and Beal M. F. (1995) Coenzyme Q10 and nicotinamide and a free radical spin trap protect against MPTP neurotoxicity. *Exp. Neurol.* **132**, 279–283.
- Takuma K., Baba A. and Matsuda T. (2004) Astrocyte apoptosis: implications for neuroprotection. *Prog. Neurobiol.* **72**, 111–127.
- The Huntington's Disease Collaborative Research Group (1993) A novel gene containing a trinucleotide repeat that is expanded and unstable on Huntington's disease chromosomes. *Cell* **72**, 971–983.
- Warrick J. M., Chan H. Y., Gray-Board G. L., Chai Y., Paulson H. L. and Bonini N. M. (1999) Suppression of polyglutamine-mediated neurodegeneration in *Drosophila* by the molecular chaperone HSP70. *Nat. Genet.* **4**, 425–428.
- West M. J., Slomianka L. and Gundersen H. J. (1991) Unbiased stereological estimation of the total number of neurons in the subdivisions of the rat hippocampus using the optical fractionator. *Anat. Rec.* **231**, 482–497.
- Westerheide S. D., Bosman J. D., Mbadugha B. N., Kawahara T. L., Matsumoto G., Kim S., Gu W., Devlin J. P., Silverman R. B. and Morimoto R. I. (2004) Celastrols as inducers of the heat shock response and cytoprotection. *J. Biol. Chem.* [Epub ahead of print].
- Yenari M. A. (2002) Heat shock proteins and neuroprotection. *Adv. Exp. Med. Biol.* **513**, 281–299.



ELSEVIER

## Neurobiology of Disease

www.elsevier.com/locate/ynbdi  
Neurobiology of Disease xx (2005) xxx – xxx

# Promethazine protects against 1-methyl-4-phenyl-1,2,3,6-tetrahydropyridine neurotoxicity

Carine Cleren,<sup>\*,1</sup> Anatoly A. Starkov,<sup>1</sup> Noel Y. Calingasan, Beverly J. Lorenzo,  
Junya Chen, and M. Flint Beal

Department of Neurology and Neuroscience, Weill Medical College of Cornell University, 525 East 68th Street, Room A-501, New York, NY 10021, USA

Received 28 February 2005; revised 26 April 2005; accepted 2 May 2005

Promethazine (PMZ) is an FDA-approved antihistaminergic drug that was identified as a potentially neuroprotective compound in the NINDS screening program. PMZ accumulates in brain mitochondria *in vivo* and inhibits  $\text{Ca}^{2+}$ -induced mitochondrial permeability transition pore (PTP) in rat liver mitochondria *in vitro*. We hypothesized that PMZ may have a protective effect in a mitochondrial toxin model of Parkinson's disease (PD). Mice treated with 1-methyl-4-phenyl-1,2,3,6-tetrahydropyridine (MPTP) sustained a significant loss of dopaminergic neurons within the SNpc that was strongly attenuated by PMZ treatment. However, neither striatal MPP<sup>+</sup> concentrations nor MPTP-induced inhibition of mitochondrial complex I were affected by PMZ treatment. In isolated mouse brain mitochondria, PMZ partially prevented and reversed MPP<sup>+</sup>-induced depolarization of membrane potential and inhibited the  $\text{Ca}^{2+}$ -induced PTP in brain mitochondria. The sum of data indicates that PMZ is a strong neuroprotective agent capable of protecting dopaminergic neurons against MPTP toxicity *in vivo*.

© 2005 Elsevier Inc. All rights reserved.

**Keywords:** Promethazine; MPTP; MPP<sup>+</sup>; Parkinson; Neuroprotection; Mitochondria; Permeability transition pore; Membrane potential; Complex I; Mice

## Introduction

Parkinson's disease (PD) is a progressive disorder leading to degeneration of a large number of dopaminergic neurons in the substantia nigra pars compacta (SNpc), which results in depletion of dopamine (DA) in the striatum (Hornykiewicz, 1966). The causes of PD remain unidentified but substantial evidence suggests an etiology involving both environmental and genetic factors (Moore et al., 2004; Greenamyre and Hastings, 2004). Administration of the mitochondrial complex I inhibitor MPTP, in

primates and rodents, reproduces the characteristic degeneration of nigrostriatal dopaminergic neurons with a depletion of striatal dopamine levels (Heikkila et al., 1984). Both mitochondrial dysfunction and oxidative stress appear to play a role in the pathogenesis of Parkinson's disease (Beal, 2003; Blum et al., 2001).

PMZ is a clinically approved drug that could readily be moved to late-stage preclinical trials and then into clinical trials. It was identified as a neuroprotective compound as part of the NINDS program to screen 1040 FDA-approved compounds in a variety of high-throughput assays (Stavrovskaya et al., 2004). Promethazine protected primary neuronal cultures subjected to oxygen/glucose deprivation and reduced infarct size and neurological impairments in mice subjected to middle cerebral artery occlusion/reperfusion (Stavrovskaya et al., 2004). In experiments with isolated rat liver mitochondria, PMZ delayed the  $\text{Ca}^{2+}$ -induced mitochondrial permeability transition pore (PTP) without impairing mitochondrial physiology (Stavrovskaya et al., 2004). In brain cells, *in vivo*, PMZ has been shown to accumulate into mitochondria and vesicles (Muller, 1996). We examine the neuroprotective effects of PMZ treatment in the MPTP model of Parkinson's disease. We found a strong neuroprotective effect and *in vitro* experiments led us to hypothesize that PMZ may be neuroprotective due to its stabilizing effects on mitochondria.

## Material and methods

### Reagents

All reagents were purchased from Sigma (St. Louis, USA). Promethazine and MPTP were dissolved in phosphate-buffered saline (PBS).

### Animals and procedures

The experiments were carried out on mice, in accordance with the NIH Guide for the Care and Use of Laboratory Animals. All

\* Corresponding author. Fax: +1 212 746 8276.

E-mail address: cac2005@med.cornell.edu (C. Cleren).

<sup>1</sup> Authors contributed equally to this study.

Available online on ScienceDirect (www.sciencedirect.com).

procedures were approved by the local Animal Care and Use Committee. Male Swiss Webster mice (12 weeks old, 4 per cage) were maintained in a temperature/humidity-controlled environment under a 12-h light/dark cycle with free access to food and water.

#### MPTP treatments

##### Protocol 1

Experiments involving measurements of neurodegeneration (TH, Nissl, DA) required sacrificing mice 7 days after treatment in order to observe the total cell death and to avoid later compensatory effects. A preliminary dose effect showed that an injection of a 5-mg/kg/dose of PMZ, twice a day, was insufficient to protect against MPTP-induced decrease in DA levels, while the 10-, 20-, and 40-mg/kg/dose were protective (Fig. 1A). Conse-

quently, mice (9–12 per group) were injected with the lowest dose of PMZ that showed protection (10 mg/kg ip) or with PBS (10 ml/kg ip) 1 h before and 12 h after the first MPTP injection. Mice were treated with MPTP (10 mg/kg ip q 2 h  $\times$  4 doses) according to a standard dosage protocol (Schmidt and Ferger, 2001) or with PBS (10 ml/kg). Mice were sacrificed 7 days later by cervical dislocation.

##### Protocol 2

In order to determine if PMZ disturbed MPTP metabolism, we examined the time course of changes in MPP<sup>+</sup> striatal concentrations following PMZ treatment. We used the highest concentration of PMZ (40 mg/kg ip) that protected against MPTP-induced DA depletion in our preliminary experiment. Mice (9–12 per group) were injected with PMZ (40 mg/kg ip) 1 h before a

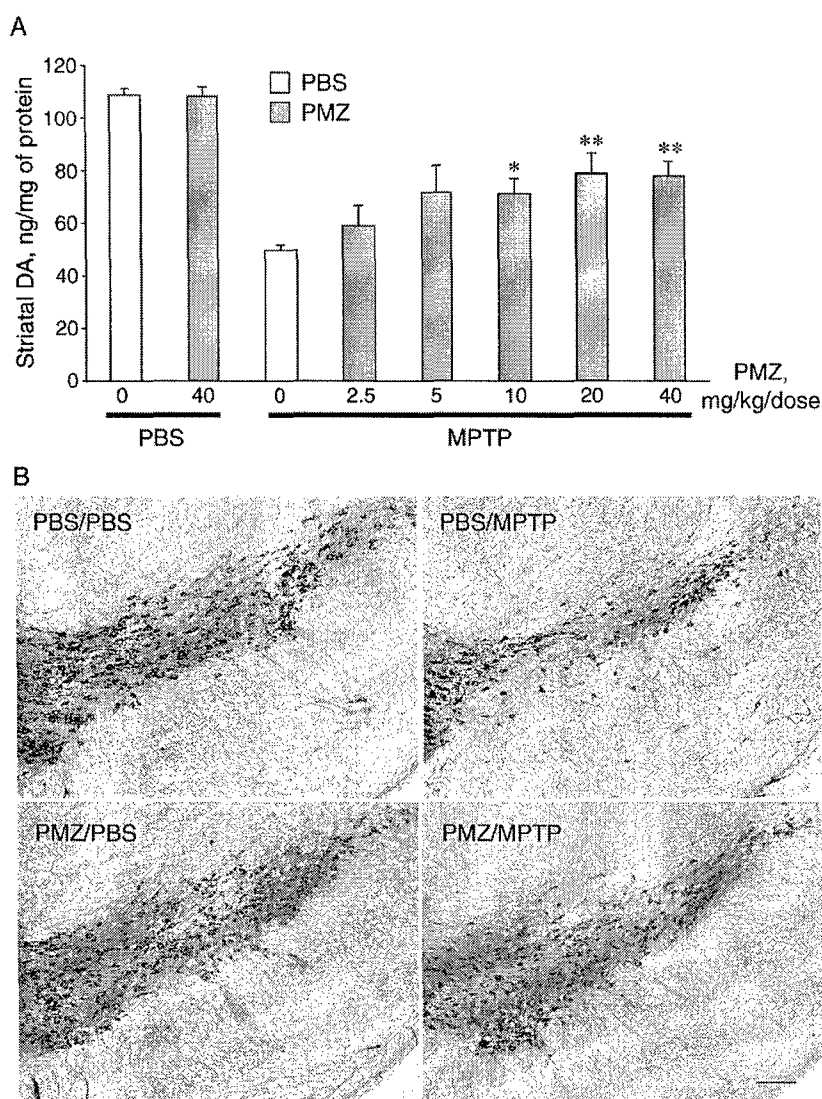


Fig. 1. Effects of PMZ treatment on striatal DA and nigral TH levels induced by MPTP treatment. (A) Injection of a 5 mg/kg/dose of PMZ, twice a day, was insufficient to protect against MPTP-induced decrease in DA levels, while the 10, 20, and 40 mg/kg/dose were protective. (B) TH immunoreactivity in the substantia nigra pars compacta of control or MPTP-lesioned mice treated with either PBS or PMZ. MPTP treatment (10 mg/kg/dose) produced a significant loss of TH-immunoreactive neurons in the substantia nigra pars compacta, while PMZ significantly mitigated the MPTP-induced loss of TH-positive neurons. Scale bar, 100  $\mu$ m.

single MPTP injection (30 mg/kg ip). Mice were sacrificed 1, 2, 4, and 8 h later.

### Protocol 3

MPTP-induced inhibition of complex I is an early and transient event (Sriram et al., 1997; Kenchappa and Ravindranath, 2003). Therefore, experiments involving measurements of complex I activity required us to sacrifice mice 15 min after the treatments. Mice (12–16 per group) were injected with PMZ (40 mg/kg ip) or PBS (10 ml/kg) 1 h before the first MPTP (10 mg/kg ip q 2 h  $\times$  4 doses) or PBS (10 ml/kg) injection. Mice were sacrificed 15 min after the last MPTP injection by cervical dislocation.

Mouse brain mitochondria were isolated by the Percoll gradient separation method as described (Sims, 1990) with minor modifications as follows. Animals were decapitated, the brain excised and placed into ice-cold isolation buffer containing 225 mM mannitol, 75 mM sucrose, 5 mM HEPES–KOH (pH 7.4), 1 mM EGTA, and 1 g/l bovine serum albumin. The cerebellum was removed, and the rest of the brain tissue was placed in a 15-ml Dounce homogenizer and homogenized manually with 8 strokes of pestle A followed by 8 strokes of pestle B. The brain homogenate was centrifuged at  $1250 \times g$  for 3 min; pellet was discarded and the supernatant was centrifuged at  $14,000 \times g$  for 10 min. The pellet was resuspended in 15% Percoll (Sigma, St. Louis, MO, USA) and layered on a preformed Percoll gradient (40% and 23%). Following centrifugation at  $30,000 \times g$  for 12 min, the mitochondrial fraction located at the interface of the lower two layers was removed, diluted with isolation buffer, and centrifuged at  $14,000 \times g$  for 10 min. The supernatant was discarded, and the loose pellet was resuspended in isolation buffer and centrifuged at  $6700 \times g$  for 10 min. The resulting pellet was suspended in 100  $\mu$ l of isolation medium devoid of EGTA.

### HPLC

For measurement of striatal dopamine or  $MPP^+$  levels, dissected striata were immediately frozen on dry ice, and stored at  $-80^\circ\text{C}$ . One striatum was sonicated and centrifuged in chilled 0.1 M perchloric acid (about 100  $\mu$ l/mg tissue).

For measurements of dopamine, the supernatant was taken and analyzed by HPLC as modified from our previously described method (Beal et al., 1990). Ten microliters of supernatant was isocratically eluted through an  $80 \times 4.6$  mm C18 column (ESA, Inc. Chelmsford, MA) with a mobile phase containing 75 mM of  $\text{NaH}_2\text{PO}_4$ , 1.5 mM OSA, 5% acetonitrile, pH 3, and detected by a two-channel Coulchem II electrochemical detector (ESA, Inc. Chelmsford, MA). The flow rate was 1 ml/min. Concentrations of dopamine were expressed as nanograms per milligram of protein. The protein concentrations of tissue homogenates were measured with the Bio-Rad protein analyze protocol (Bio-Rad Laboratories, Hercules, CA) and HTS7000+ plate reader (Perkin Elmer, Norwalk, CT).

For measurements of  $MPP^+$ , the supernatant was taken and analyzed by HPLC using a  $4.6 \text{ mm} \times 250 \text{ mm}$  Waters Xterra MSC18 5  $\mu$ m column, Waters 515 pump, and a Waters 474 Scanning Fluorometer set at 295 nm excitation and 375 nm emission. The mobile phase was a pH 8.0, 20 mM borate buffer containing 3 mM tetrabutylammonium hydrogen sulfate and 0.25 mM 1-heptanesulfonic acid with 10% isopropanol (Naoi et al., 1987). Concentrations of  $MPP^+$  are expressed as nanograms per milligram of wet tissue.

### Histological and stereological analyses

#### Immunohistochemistry

Fresh brains were fixed by immersion in 4% paraformaldehyde (PFA) overnight at  $4^\circ\text{C}$ . Prior to sectioning, the tissues were placed in 30% glucose overnight at  $4^\circ\text{C}$  for cryoprotection. Serial coronal sections (50  $\mu$ m thick) were cut through the substantia nigra or the striatum using a cryostat. Two sets consisting of eight sections each, 100  $\mu$ m apart, were prepared. One set of sections was used for Nissl staining, and the other was processed for tyrosine hydroxylase (TH) immunohistochemistry using the avidin–biotin peroxidase technique (Vectastain ABC kit from Vector Labs, Burlingame, CA). A rabbit anti-TH affinity purified antibody (Chemicon, Temecula, CA; 1:3000) was used. The numbers of Nissl-stained or TH-immunoreactive cells in both sides of the substantia nigra pars compacta (SNpc) were estimated using the optical fractionator (West and Gundersen, 1990). Analysis was performed using a system consisting of a Nikon Eclipse E600 microscope equipped with a computer-controlled LEP BioPoint motorized stage, a DEI-750 video camera, a Dell Dimension 4300 computer, and the Stereo Investigator (v. 4.35) software program (MicroBrightfield, Burlington, VT). Tissue sections were examined using a Nikon Plan Apo 100 $\times$  objective lens with a 1.4 numerical aperture. The size of the  $x$ – $y$  sampling grid was 140  $\mu$ m. The counting frame thickness was 14  $\mu$ m and the counting frame area was  $4900 \mu\text{m}^2$ . The coefficient of error and coefficient of variation were also determined.

#### Enzyme assays

Complex I activity was measured spectrophotometrically as rotenone-sensitive NADH: $Q_1$  reductase. Reaction buffer was composed of 10 ml 2 mM HEPES (pH 7.8), 75  $\mu$ M NADH, and 40  $\mu$ M coenzyme  $Q_1$  (final concentration). Frozen–thawed mice striata were homogenized in 2 mM HEPES buffer (pH 7.8) mixed with the reaction buffer in a 96-well plate and the absorbance changes at 340 nm were followed for 15 min with a plate reader HTS7000+ (Perkin Elmer, Norwalk, CT). In control incubations the reaction buffer was supplemented with 2  $\mu$ M rotenone (final concentration). The activity of complex I was calculated as the difference between the rates of NADH oxidation ( $E^{340} \text{ mM} = 6.22 \text{ cm}^{-1}$ ) in the absence and in the presence of rotenone and presented in nanomoles NADH per minute per milligram of wet tissue (Starkov and Fiskum, 2003).

Aconitase activity was measured spectrophotometrically by following the appearance of NADPH at 340 nm (Gardner, 2002). Reaction buffer was composed of 2 mM HEPES (pH 7.8), 0.6 mM  $\text{MnCl}_2$ , 0.5 mM  $\text{NADP}^+$ , 2 units of isocitrate dehydrogenase, 1  $\mu$ M rotenone, 10  $\mu$ M  $\text{CaCl}_2$ , and 1 mM citrate. Frozen–thawed rat cortex samples were homogenized in 2 mM HEPES buffer (pH 7.8) and mixed with the reaction buffer in a 96-well plate and the absorbance changes at 340 nm were followed for 15 min with a plate reader HTS7000+ (Perkin Elmer, Norwalk, CT).

Membrane potential ( $\Delta\Psi$ ) of isolated mitochondria was estimated using the fluorescence of safranin O with excitation and emission wavelengths of 495 nm and 586 nm, respectively (Starkov et al., 2002). Incubation medium was composed of 125 mM KCl, 14 mM NaCl, 2 mM  $\text{KH}_2\text{PO}_4$ , 5 mM HEPES (pH 7.2), 4 mM  $\text{MgCl}_2$ , 3 mM ATP, 7 mM Pyruvate, 1 mM malate, and 2.5  $\mu$ M safranin O,  $t = 37^\circ\text{C}$ . Mouse brain mitochondria were added at 0.125 mg/ml, other

additions were as indicated in legends to figures. Fluorescence of safranin O was measured with an F4500 fluorimeter (Hitachi, Japan) equipped with a magnetic stirring assembly and a thermostated cuvette holder.

Mitochondrial permeability transition pore was assessed by monitoring the  $\text{Ca}^{2+}$  retention and the swelling of mitochondria. Incubation medium was composed of 250 mM sucrose, 75 mM mannitol, 5 mM HEPES (pH 7.2), 2 mM  $\text{KH}_2\text{PO}_4$ , 1 mM  $\text{MgCl}_2$ , 10 mM EGTA, 0.2  $\mu\text{M}$  Calcium Green 5N (calcium indicator), 10 mM succinate, and 1  $\mu\text{M}$  rotenone,  $t = 37^\circ\text{C}$ . Mouse brain or liver mitochondria were added at 0.25 mg/ml, other additions were as indicated in legends to figures. Changes in external  $\text{Ca}^{2+}$  were monitored as changes in Calcium Green 5N fluorescence measured at 506 nm excitation and 531 nm emission wavelengths with F4500 fluorimeter (Hitachi, Japan) equipped with a magnetic stirring assembly and a thermostated cuvette holder. Swelling of mitochondria was measured simultaneously as light scattering at 590/590 nm excitation/emission.

#### Statistical analysis

All data were computed in a database (Graphpad Instat® software) and expressed as mean  $\pm$  SEM. Differences between groups and interaction between treatments were assessed by a Student's  $t$  test (unpaired) or by a one-way analysis of variance (ANOVA) followed, when appropriate, by a Student–Newman–Keuls post hoc test. A probability level of 5% ( $P < 0.05$ ) was considered significant.

## Results

#### Promethazine diminishes MPTP-induced neural tissue damage in mice

Mice that received MPTP (Protocol 1) sustained a 39% loss ( $P < 0.001$ ) of Nissl-stained neurons (Table 1) and 37% ( $P < 0.01$ ) loss of tyrosine hydroxylase (TH) immunopositive dopaminergic neurons within the SNpc, compared to sham-injected (PBS) mice (Table 1 and Fig. 1B). MPTP treatment decreased striatal dopamine levels by 43% ( $P < 0.001$ ; Table 1).

Table 1

Effects of PMZ treatment on MPTP-induced neurotoxicity

	Nissl (average $\pm$ SEM)	TH (average $\pm$ SEM)	DA (average $\pm$ SEM)
PBS/PBS	12818.5 $\pm$ 678	9805.1 $\pm$ 616	103.0 $\pm$ 3
PMZ/PBS	12079.0 $\pm$ 384	9865.7 $\pm$ 522	97.4 $\pm$ 4
PBS/MPTP As compared to PBS/PBS	7758.6 $\pm$ 523, $P < 0.001$	6341.5 $\pm$ 777, $P < 0.01$	58.7 $\pm$ 6, $P < 0.001$
PMZ/MPTP As compared to PBS/MPTP	9960.0 $\pm$ 480, $P < 0.05$	8951.5 $\pm$ 649, $P < 0.01$	81.2 $\pm$ 5, $P < 0.01$

Total number of neurons in both sides of the substantia nigra pars compacta (SNpc) estimated after Nissl staining (cell body); total number of dopaminergic neurons in the SNpc counted after TH (tyrosine hydroxylase) immunohistochemistry; striatal level (ng/mg of protein) of dopamine (DA) measured by HPLC. Mice were sacrificed 7 days after treatments. PMZ protected against MPTP-induced depletion of these 3 parameters.

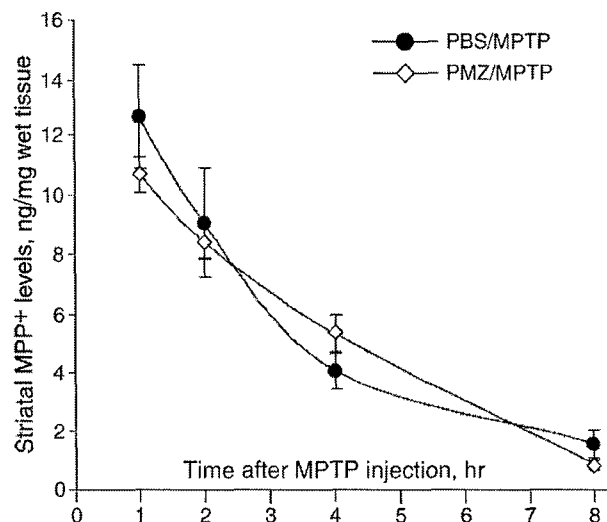


Fig. 2. Effects of PMZ pretreatment on striatal  $\text{MPP}^+$  levels induced by MPTP treatment. Mice were sacrificed 1, 2, 4, or 8 h after the first MPTP injection. PMZ treatment did not influence striatal  $\text{MPP}^+$  levels resulting from the MPTP injection. Striatal  $\text{MPP}^+$  levels diminished quickly and were nearly negligible 8 h after the injection.

Promethazine treatment (10 mg/kg ip q 12 h  $\times$  2 doses) significantly diminished the MPTP-induced loss of SNpc neurons. Indeed, PMZ protected Nissl-stained neurons ( $P < 0.05$ ; Table 1) and TH-positive neurons ( $P < 0.01$ ; Table 1 and Fig. 1B). PMZ also significantly protected against MPTP-induced depletion of striatal dopamine ( $P < 0.01$ ; Table 1).

#### Promethazine does not affect the dynamic of $\text{MPP}^+$ retention in mouse striata

The toxic metabolite of MPTP,  $\text{MPP}^+$ , accumulates in brain mitochondria (Ramsay and Singer, 1986) as does PMZ (Muller, 1996). Therefore, it was interesting to examine both the time dependence of  $\text{MPP}^+$  retention in mouse striata, and the effect of PMZ treatment on it. For these experiments, mice were treated with MPTP and PMZ (Protocol 2) and sacrificed 1, 2, 4, and 8 h after the MPTP injection. The striata were excised and frozen at  $-80^\circ\text{C}$ . Frozen tissue was later thawed and used for measurements of  $\text{MPP}^+$  content and total aconitase activity. Fig. 2 shows that PMZ treatment did not affect  $\text{MPP}^+$  retention in mouse striata. Almost all  $\text{MPP}^+$  was gone from the tissue by 8 h. Both the initial concentrations of  $\text{MPP}^+$  in mouse tissue and the time course of its removal are in a good agreement with other studies utilizing similar MPTP treatment protocols (Liang and Patel, 2004).

#### Promethazine does not protect against MPTP-induced inhibition of mitochondrial complex I

MPTP is a well-known mitochondrial toxin targeting complex I (Nicklas et al., 1985) of the respiratory chain. We therefore examined the effect of PMZ treatment on mitochondrial enzyme activities in MPTP-treated mice.

MPTP inhibition of complex I in MPTP-treated mice was previously shown to be a transient event (Sriram et al., 1997; Kenchappa and Ravindranath, 2003). Therefore, we sacrificed animals 15 min after the MPTP injection (Protocol 3). This

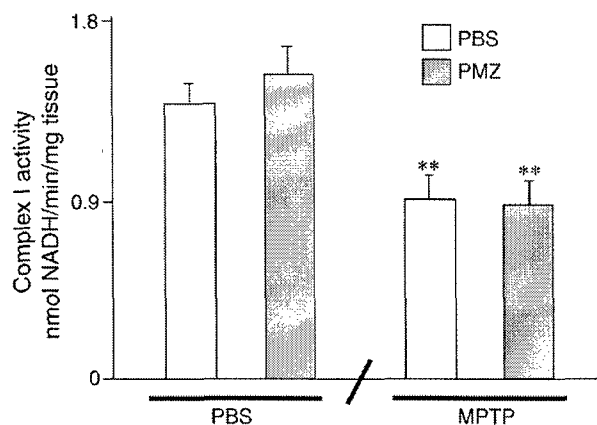


Fig. 3. Effect of PMZ treatment on MPTP-induced complex I inhibition in mice striatum. Mice were sacrificed 15 min after the last MPTP injection.  $**P < 0.001$  as compared to PBS/PBS-treated rats.

protocol yielded a significant inhibition of complex I activity in mice striata. PMZ treatment did not prevent complex I inhibition (Fig. 3).

#### Promethazine prevents MPTP-induced transient inhibition of aconitase in mouse striatum

Aconitase activity is very sensitive to inhibition by superoxide and therefore considered to be a good in vivo tissue marker of oxidative stress (Gardner, 2002). MPTP treatment (Protocol 2) resulted in a transient inhibition of total aconitase activity in mouse striata 2 h after MPTP injection ( $P < 0.05$ ), which was significantly reversed by the PMZ treatment ( $P < 0.05$ ). However, since the 2-h activity in PBS/MPTP-treated mice is similar to the 4-h activity of PMZ/MPTP-treated mice, we cannot exclude the hypothesis that PMZ treatment may only delay MPTP-induced depression in aconitase activity (Fig. 4).

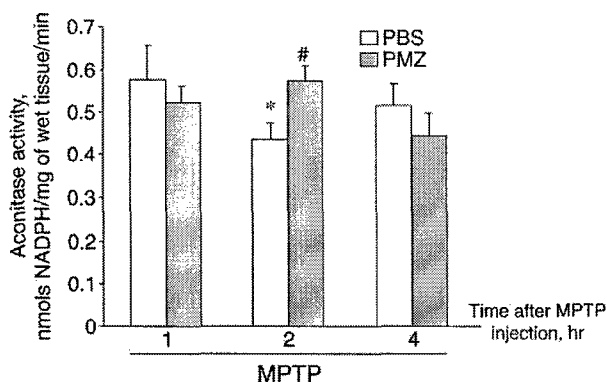


Fig. 4. Effects of PMZ treatment on MPTP-induced inhibition of aconitase activity. Mice were sacrificed 1, 2, or 4 h after the first MPTP injection. Two hours after MPTP treatment aconitase activity was transiently inhibited. PMZ treatment prevented the MPTP-induced aconitase inhibition.  $*P < 0.05$  as compared to PBS/MPTP-treated rats 1 h after the MPTP injection;  $\#P < 0.05$  as compared to PBS/MPTP-treated rats 2 h after the MPTP injection.

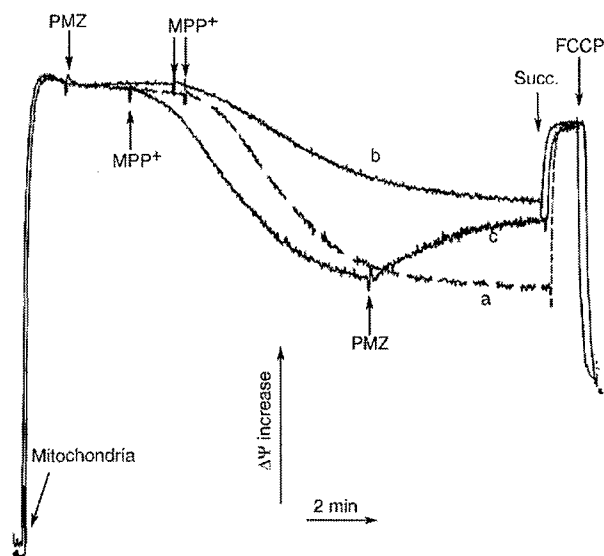


Fig. 5. Effect of PMZ and MPP<sup>+</sup> additions on mitochondrial membrane potential. Isolated brain mitochondria were incubated in a cytosolic-like medium: PMZ (125  $\mu$ M) both attenuated (curve b) and reversed (curve c) MPP<sup>+</sup> (200  $\mu$ M)-induced mitochondrial membrane depolarization (curve a).

#### Promethazine both attenuated and reversed MPP<sup>+</sup>-induced mitochondrial membrane depolarization in vitro

The toxicity of MPTP in vivo is thought to be at least partially due to the inhibitory effect of its metabolite, MPP<sup>+</sup>, on mitochondrial complex I (Nicklas et al., 1985). It is well established that in vitro, MPP<sup>+</sup> inhibits the respiration of brain mitochondria supported by a complex I-related NAD<sup>+</sup>-linked substrates such as pyruvate and malate (Mizuno et al., 1988); however, the effect of MPP<sup>+</sup> on the mitochondrial membrane potential has not yet been reported. We examined both the effect of MPP<sup>+</sup> and PMZ on the membrane potential and the respiration of

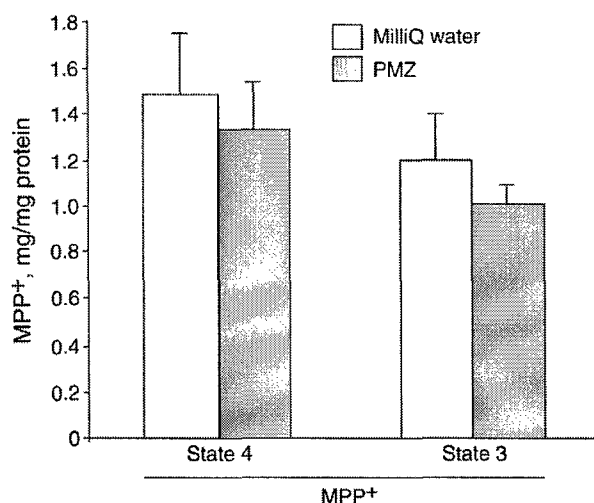


Fig. 6. Effect of PMZ on MPP<sup>+</sup> accumulation in mitochondria during active and resting states. Brain mitochondria were incubated with MPP<sup>+</sup> (200  $\mu$ M) in the presence or in the absence of PMZ (125  $\mu$ M). PMZ did not affect MPP<sup>+</sup> accumulation by mitochondria in either resting state (state 4) or active (phosphorylating: state 3).

mouse brain mitochondria. Isolated mitochondria were incubated in a cytosol-like high ionic strength medium supplemented with pyruvate and malate. The addition of 200  $\mu\text{M}$   $\text{MPP}^+$  induced a slow depolarization of mitochondria (Fig. 5, curve a). The slow dynamic of  $\text{MPP}^+$ -induced depolarization of mitochondria is most likely due to the slow penetration of  $\text{MPP}^+$  through the mitochondrial membrane to its target site in the complex I (Ramsay and Singer, 1986). The addition of PMZ had no effect on the membrane potential. PMZ added in the medium either before or after  $\text{MPP}^+$ , partially attenuated (Fig. 5, curve b) and reversed (Fig. 5, curve c) respectively  $\text{MPP}^+$ -induced mitochondrial membrane depolarization. The addition of succinate to  $\text{MPP}^+$ -depolarized mitochondria restored the membrane potential, thereby indicating that the decrease was indeed due to the inhibition of

complex I or  $\text{NAD}^+$ -linked primary substrate dehydrogenases, and not due to an uncoupling or membrane damage induced by  $\text{MPP}^+$  accumulation.

As described above, PMZ alone had no effect on the mitochondrial membrane potential. However, it was possible that PMZ, which can be accumulated in mitochondria (Muller, 1996), interfered with  $\text{MPP}^+$  accumulation, thereby decreasing the effective  $\text{MPP}^+$  concentration in mitochondria. Therefore, we measured  $\text{MPP}^+$  accumulation in mitochondria. For this purpose, mitochondria were incubated with 200  $\mu\text{M}$   $\text{MPP}^+$  in the absence or in the presence of 125  $\mu\text{M}$  PMZ. When present, PMZ was added 2 min before  $\text{MPP}^+$ . PMZ did not affect  $\text{MPP}^+$  accumulation by mitochondria in either active (phosphorylating) or resting states (Fig. 6).

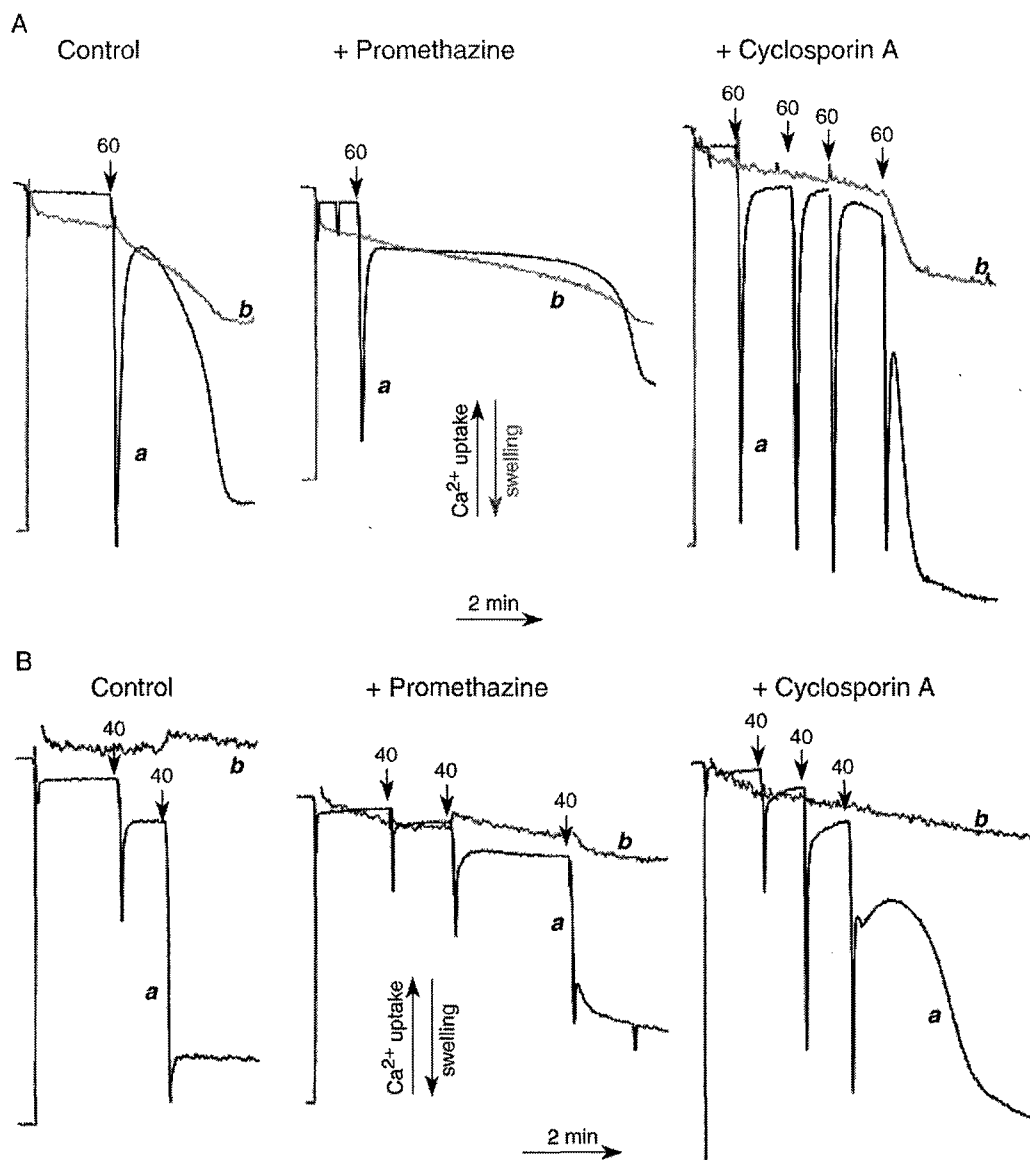


Fig. 7. Effect of PMZ on mitochondrial calcium capacity. (A) Isolated liver mitochondria were incubated in a mannitol/sucrose medium. PMZ (10  $\mu\text{M}$ ) increased the calcium capacity threshold for the mitochondrial permeability transition pore (middle panel) to a similar extent as cyclosporin A (0.5  $\mu\text{M}$ , right panel). Sixty nanomoles of  $\text{Ca}^{2+}$  was added per milligram of mitochondria. (B) Isolated brain mitochondria were incubated in a mannitol/sucrose medium. PMZ (10  $\mu\text{M}$ ) increased the calcium capacity threshold for the mitochondrial permeability transition pore (middle panel) to a similar extent as cyclosporin A (0.5  $\mu\text{M}$ , right panel). Forty nanomoles of  $\text{Ca}^{2+}$  was added per milligram of mitochondria.

### PMZ increased the $\text{Ca}^{2+}$ threshold for the induction of mitochondrial permeability transition

Earlier, PMZ was shown to delay the  $\text{Ca}^{2+}$ -induced mitochondrial permeability transition pore in rat liver mitochondria (Stavrovskaya et al., 2004). We found that 10  $\mu\text{M}$  PMZ significantly extended ( $\sim 3.5$  times) the lag period between the  $\text{Ca}^{2+}$  loading and the activation of the permeability transition pore in mouse liver mitochondria (Fig. 7A). The opening of the PTP was manifested as a spontaneous progressing release of accumulated  $\text{Ca}^{2+}$  (Fig. 7A, left panel, curve a) accompanied by the swelling of liver mitochondria (Fig. 7A, left panel, curve b). In the presence of promethazine, the spontaneous release of  $\text{Ca}^{2+}$  was significantly delayed (Fig. 7A, middle panel, curve a) and the swelling of liver mitochondria was less pronounced (Fig. 7A, middle panel, curve b). In liver mitochondria, cyclosporin A significantly elevated the  $\text{Ca}^{2+}$  threshold for the induction of the PTP (Fig. 7A, right panel, curves a).

Essentially similar effects were observed in experiments with isolated mouse brain mitochondria incubated under the same conditions. Promethazine increased the  $\text{Ca}^{2+}$  retention and the  $\text{Ca}^{2+}$  threshold for the induction of PTP (Fig. 7B, middle panel) with an efficiency similar to that of cyclosporin A (Fig. 7B, right panel).  $\text{Ca}^{2+}$  loading of mouse brain mitochondria under our experimental conditions did not induce swelling. This is in agreement with earlier published reports addressing the differences in response of rodent brain and liver mitochondria on  $\text{Ca}^{2+}$  challenge and PTP inhibitors, showing that brain mitochondria do not swell as liver mitochondria do (Andreyev and Fiskum, 1999; Berman et al., 2000).

### Discussion

The data presented in this manuscript allow us to conclude that PMZ is a strong neuroprotective compound capable of attenuating neurodegeneration induced by MPTP in mice. Indeed, PMZ prevented both the neurodegeneration of nigrostriatal dopaminergic neurons and the loss of striatal dopamine induced by MPTP in mice. In addition, we showed that PMZ protected isolated mouse brain mitochondria against  $\text{MPP}^+$ -induced depolarization of the membrane potential and against the  $\text{Ca}^{2+}$ -induced permeability transition.

Inhibition of complex I of the mitochondrial respiratory chain by MPTP metabolite,  $\text{MPP}^+$ , is thought to play a significant role in the molecular mechanism of MPTP-induced neurotoxicity (Przedborski and Jackson-Lewis, 1998). It is therefore quite interesting that inhibition of complex I in striatal tissue of mice treated with MPTP resolved as early as 2 h after the last MPTP injection, which is in agreement with previous publications (Sriram et al., 1997; Kenchappa and Ravindranath, 2003). However, the concentration of  $\text{MPP}^+$  in striatal tissue at this time point was still high (Fig. 2) and also in agreement with values published earlier (Sriram et al., 1997). The transient character of MPTP-induced inhibition of complex I in striatal tissue has not yet been fully explained.

PMZ treatment clearly protected brain tissue against MPTP-induced toxicity but did not rescue the activity of complex I (Fig. 3), neither did it change the retention of  $\text{MPP}^+$  in striatal tissue (Fig. 2). However, PMZ treatment protected the loss of aconitase activity seen 2 h after MPTP treatment (Fig. 4). Aconitase activity

is thought to be a marker of oxidative stress because the enzyme is inhibited by superoxide (Gardner, 2002). Therefore, our data indicate that PMZ may protect against MPTP-induced oxidative stress.

PMZ was capable of rescuing the mitochondrial membrane potential of isolated mouse brain mitochondria that was decreased by the addition of  $\text{MPP}^+$  (Fig. 5). In these experiments, 200  $\mu\text{M}$   $\text{MPP}^+$  induced a slow decrease in the membrane potential of mitochondria incubated under either non-phosphorylating conditions ("resting state", in the absence of ADP; Fig. 5, curve a) or phosphorylating conditions (data not presented). PMZ did not change the accumulation of  $\text{MPP}^+$  in brain mitochondria (Fig. 6); however, it partially attenuated (Fig. 5, curve b) and/or restored (Fig. 5, curve c) the membrane potential decrease induced by  $\text{MPP}^+$  (Fig. 5, curve a). The effect of PMZ was dose dependent, with the strongest effect at the 125- $\mu\text{M}$  concentration, shown in Fig. 5. At the concentrations used in our experiments, PMZ had no effect on the membrane potential, in agreement with an earlier study using lower concentrations of the drug (Stavrovskaya et al., 2004). The molecular mechanism of this PMZ effect is under investigation; our preliminary data indicate that PMZ affects the electron transfer reactions within complex I (Starkov et al., 2004).

Low concentrations of PMZ increased the threshold level of mitochondrial  $\text{Ca}^{2+}$  accumulation needed to induce the permeability transition pore in mouse liver (Fig. 7A) and brain mitochondria (Fig. 7B). This effect of PMZ was reported earlier with rat liver mitochondria and was thought to be responsible for tissue protection against damage induced by ischemia (Narayanan et al., 2004; Stavrovskaya et al., 2004). We confirmed the observations of these authors and extended it to both mouse liver and brain mitochondria.

The mechanism of the protective action of PMZ requires further research. In this manuscript, we describe a novel direct protective effect of PMZ on mitochondrial membrane potential and show that it inhibits activation of the PTP in brain mitochondria. The neuroprotection we observed suggests that PMZ could play a role in preventing and/or delaying the onset of PD.

### Acknowledgments

The work was supported by grants from the Department of Defense, the Michael J. Fox Foundation, and the Parkinson's Disease Foundation.

### References

- Andreyev, A., Fiskum, G., 1999. Calcium induced release of mitochondrial cytochrome c by different mechanisms selective for brain versus liver. *Cell Death Differ.* 6, 825–832.
- Beal, M.F., 2003. Bioenergetic approaches for neuroprotection in Parkinson's disease. *Ann. Neurol.* 53 (Suppl. 3), S39–S47.
- Beal, M.F., Matson, W.R., Swartz, K.J., Gamache, P.H., Bird, E.D., 1990. Kynurenine pathway measurements in Huntington's disease striatum: evidence for reduced formation of kynurenic acid. *J. Neurochem.* 55, 1327–1339.
- Berman, S.B., Watkins, S.C., Hastings, T.G., 2000. Quantitative biochemical and ultrastructural comparison of mitochondrial permeability transition in isolated brain and liver mitochondria: evidence for reduced sensitivity of brain mitochondria. *Exp. Neurol.* 164, 415–425.
- Blum, D., Torch, S., Lambeng, N., Nissou, M., Benabid, A.L., Sadoul, R.,

- Verna, J.M., 2001. Molecular pathways involved in the neurotoxicity of 6-OHDA, dopamine and MPTP: contribution to the apoptotic theory in Parkinson's disease. *Prog. Neurobiol.* 65, 135–172.
- Gardner, P.R., 2002. Aconitase: sensitive target and measure of superoxide. *Methods Enzymol.* 349, 9–23.
- Greenamyre, J.T., Hastings, T.G., 2004. Biomedicine. Parkinson's-divergent causes, convergent mechanisms. *Science* 304, 1120–1122.
- Heikkilä, R.E., Cabbat, F.S., Manzino, L., Duvoisin, R.C., 1984. Effects of 1-methyl-4-phenyl-1,2,5,6-tetrahydropyridine on neostriatal dopamine in mice. *Neuropharmacology* 23, 711–713.
- Hornykiewicz, O., 1966. Dopamine (3-hydroxytyramine) and brain function. *Pharmacol. Rev.* 18, 925–964.
- Kenchappa, R.S., Ravindranath, V., 2003. Glutaredoxin is essential for maintenance of brain mitochondrial complex I: studies with MPTP. *FASEB J.* 17, 717–719.
- Liang, L.P., Patel, M., 2004. Iron-sulfur enzyme mediated mitochondrial superoxide toxicity in experimental Parkinson's disease. *J. Neurochem.* 90, 1076–1084.
- Mizuno, Y., Sone, N., Suzuki, K., Saitoh, T., 1988. Studies on the toxicity of 1-methyl-4-phenylpyridinium ion (MPP<sup>+</sup>) against mitochondria of mouse brain. *J. Neurol. Sci.* 86, 97–110.
- Moore, D.J., West, A.B., Dawson, V.L., Dawson, T.M., 2004. Molecular pathophysiology of Parkinson's disease. *Annu. Rev. Neurosci.* (electronic publication ahead of print).
- Muller, T., 1996. Electron microscopic demonstration of intracellular promethazine accumulation sites by a precipitation technique: application to the cerebellar cortex of the mouse. *J. Histochem. Cytochem.* 44, 531–535.
- Naoi, M., Takahashi, T., Nagatsu, T., 1987. A fluorometric determination of *N*-methyl-4-phenylpyridinium ion, using high-performance liquid chromatography. *Anal. Biochem.* 162, 540–545.
- Narayanan, M.V., Zhang, W., Stavrovskaya, I.G., Kristal, B.S., Friedlander, R.M., 2004. Promethazine: a novel application as a neuroprotectant that reduces ischemia-mediated injury by inhibiting mitochondrial dysfunction. *Clin. Neurosurg.* 51, 102–107.
- Nicklas, W.J., Vyas, I., Heikkilä, R.E., 1985. Inhibition of NADH-linked oxidation in brain mitochondria by 1-methyl-4-phenyl-pyridine, a metabolite of the neurotoxin, 1-methyl-4-phenyl-1,2,5,6-tetrahydropyridine. *Life Sci.* 36, 2503–2508.
- Przedborski, S., Jackson-Lewis, V., 1998. Mechanisms of MPTP toxicity. *Mov. Disord.* 13 (Suppl. 1), S35–S38.
- Ramsay, R.R., Singer, T.P., 1986. Energy-dependent uptake of *N*-methyl-4-phenylpyridinium, the neurotoxic metabolite of 1-methyl-4-phenyl-1,2,3,6-tetrahydropyridine, by mitochondria. *J. Biol. Chem.* 261, 7585–7587.
- Schmidt, N., Feger, B., 2001. Neurochemical findings in the MPTP model of Parkinson's disease. *J. Neural. Transm.* 108, 1263–1282.
- Sims, N.R., 1990. Rapid isolation of metabolically active mitochondria from rat brain and subregions using Percoll density gradient centrifugation. *J. Neurochem.* 55, 698–707.
- Sriram, K., Pai, K.S., Boyd, M.R., Ravindranath, V., 1997. Evidence for generation of oxidative stress in brain by MPTP: in vitro and in vivo studies in mice. *Brain Res.* 749, 44–52.
- Starkov, A.A., Fiskum, G., 2003. Regulation of brain mitochondrial H<sub>2</sub>O<sub>2</sub> production by membrane potential and NAD(P)H redox state. *J. Neurochem.* 86, 1101–1107.
- Starkov, A.A., Polster, B.M., Fiskum, G., 2002. Regulation of hydrogen peroxide production by brain mitochondria by calcium and Bax. *J. Neurochem.* 83, 220–228.
- Starkov, A.A., Cleren, C., Beal, M.F., 2004. Promethazine may protect brain mitochondria against toxins by ensuring the NADH oxidation by complex I. *Neuroscience Meeting, Program*, 485.5.
- Stavrovskaya, I.G., Narayanan, M.V., Zhang, W., Krasnikov, B.F., Heemskerk, J., Young, S.S., Blass, J.P., Brown, A.M., Beal, M.F., Friedlander, R.M., Kristal, B.S., 2004. Clinically approved heterocyclics act on a mitochondrial target and reduce stroke-induced pathology. *J. Exp. Med.* 2004, 211–222.
- West, M.J., Gundersen, H.J., 1990. Unbiased stereological estimation of the number of neurons in the human hippocampus. *J. Comp. Neurol.* 296, 1–22.